Measuring synaptic vesicles using cellular electrochemistry and nanoscale molecular imaging

Nhu T. N. Phan[1,2], Xianchan Li[1] and Andrew G. Ewing[1,3]

Abstract | The synaptic vesicle, a cellular compartment tens to hundreds of nanometres in size, is a main player in the process of exocytosis for neuronal communication. Understanding the regulatory mechanism of neurotransmission and neurological disorders requires the quantification of chemicals transmitted between cells. These challenging single vesicle measurements can be performed using analytical techniques described in this Review. *In vivo* amperometry at living cells can be used to quantify the amount of neurotransmitter released from a vesicle. By contrast, intracellular vesicle impact electrochemical cytometry allows the amount of molecules to be determined inside single vesicles. Although the dominant mode of exocytosis from vesicles is still under debate, several experiments point to the importance of partial release modes. Making use of fluorescent or isotopically labelled probes enables super-resolution optical and mass spectrometric imaging of molecular composition and activity of single vesicles. Correlating results from these nanoscopic techniques with those from electrochemistry has proved advantageous in understanding the relationship between vesicle structure and function.

Neurotransmission within the brain is enabled by synaptic vesicles, small spherical organelles that are responsible for the storage and stimulated release of neurotransmitters between neurons (BOX 1). Occurring through synapses, exocytosis, uptake and recycling events are necessary for continuous neurotransmission cycles. These vesicle processes must be carefully coordinated and the vesicles must be particularly well organized to facilitate their synaptic functions and regulate neuronal communication. Within neuroscience and neurobiology, importance is placed on studying synaptic vesicles — both in terms of their properties and the chemical mechanisms by which they function — for an insight into brain function. The considerable gaps in our understanding provide opportunities for chemists, armed with newly developed analytical techniques, to help construct a detailed molecular-level paradigm.

Individual synaptic vesicles are small (~40–50 nm for small synaptic vesicles and 100–300 nm for dense core vesicles) and cannot be easily studied using conventional analytical methods, which have insufficient spatial and temporal resolution, sensitivity and specificity. Much of our knowledge of vesicles comes from extensive lipidomics and proteomics studies using in-solution mass spectrometry, a bulk method that provides no information of molecular organization at the single-vesicle level. Nevertheless, liquid chromatography–mass spectrometry does afford detailed information regarding the protein and lipid compositions of the synaptic vesicle[1]. In this case, the mole fractions of the different phospholipids and fatty acids are determined relative to the amount of protein per vesicle. The different proteins can be separated using 2D polyacrylamide gel electrophoresis, and subsequent identification by mass spectrometry reveals the protein composition of the vesicles[2]. The proteins can also be imaged inside cells using confocal microscopy, after the introduction of antibody fluorescence probes and green fluorescence proteins (GFPs)[3,4]. However, the diffraction limit has precluded the acquisition of vesicle images with sufficient spatial resolution using this technique.

Measuring vesicles and synaptic activities

Electrochemistry. Electrochemistry of single cells can allow quantification of important electroactive molecules (including dopamine, serotonin, adrenaline, noradrenaline and histamine) present in single vesicles and exocytosis events. The analyte molecules can be detected at femto- to zeptomole levels with temporal resolutions from microseconds to milliseconds. Despite the high sensitivity and speed of the biosensors now at our disposal, efforts are still being made to improve the selectivity of these probes and their ability to measure a wider range

[1]*University of Gothenburg, Department of Chemistry and Molecular Biology, Gothenburg 41296, Sweden.*
[2]*University of Göttingen Medical Center, Institute of Neuro- and Sensory Physiology, Göttingen 37073, Germany.*
[3]*Chalmers University of Technology, Department of Chemistry and Chemical Engineering, Gothenburg 41296, Sweden.*

Correspondence to A.G.E.
andrew.ewing@chem.gu.se

doi:10.1038/s41570-017-0048
Published online 7 Jun 2017

© 2017 Macmillan Publishers Limited, part of Springer Nature. All rights reserved.

Box 1 | **Neurotransmission by synaptic vesicles**

Neurons in the brain are specialized cells that have a central body in which the cell nucleus and transport systems reside. Peripheral to this 'control centre' are branches or processes believed to carry signals into or away from the cell, the structures responsible for this being termed dendrites and axons, respectively (part **a**). When two neurons contact each other, the transfer of molecules is triggered by changes in membrane potential — termed action potentials — whereby the axon of one cell communicates with the dendrite of another across a nanometre-scale space called a synapse. The primary means of communication is by release of transmitter molecules stored in membranous vesicles tens to hundreds of nanometres in size (part **b**). These structures are equipped with proteins on their surface to bind to the cell membrane and form a fusion pore through which the stored molecules can be released. On release, these molecules go into the synapse and affect the receptors present, thus initiating or inhibiting neuronal signals.

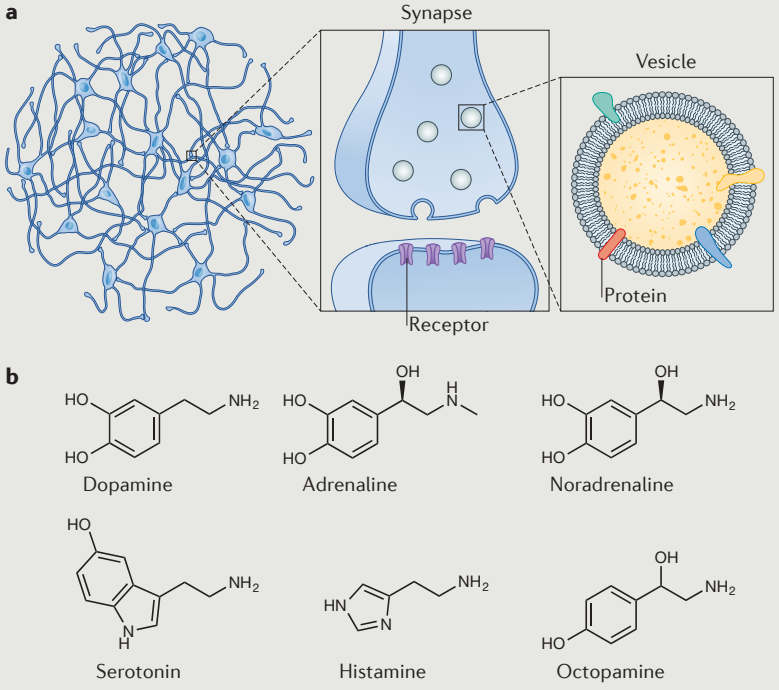

of neurotransmitters. Rather than discussing such engineering aspects, we now introduce the two main methods of electrochemistry — single-cell amperometry and intracellular vesicle impact electrochemical cytometry (VIEC)[5,6] — that have contributed to our knowledge of the exocytosis mechanism and the different factors affecting the process[7,8].

Single-cell amperometry enables the detection of neurotransmitters released from a single synaptic vesicle during exocytosis. This technique typically involves placing a carbon fibre working microelectrode in close proximity to a cell, with a reference electrode stationed nearby in the surrounding solution. Fortunately, the magnitude of the current i measured is only very small, such that the resulting potential is unaffected by the negligible potential drop ($\Delta V = iR$) across a solution of resistance R. Indeed, accurate placement of the reference electrode is not crucial and an auxiliary electrode is not needed. When a constant potential difference exists between the working and references electrodes, the working electrode can oxidize molecules secreted from a vesicle docked at the cell membrane. Such events are observed in the form of current 'transients', which appear as spikes in a plot of current versus time. Integrating the signals gives the total charge transferred Q, which is related to the number of moles of neurotransmitter released N according to Faraday's law: $N = Q/n'F$, where n' is the number of electrons removed from each analyte molecule and $F = 96{,}485\ C\ mol^{-1}$. Although the area under the current transient corresponds to the quantity of neurotransmitter released, the shape of the signal is related to the release dynamics, a subject we address in later sections.

The second major electrochemical technique covered in this Review is intracellular VIEC, which can be used to measure the total redox-active neurotransmitter content of single vesicles in the cytoplasm. This experiment involves penetrating the cell membrane with a nanotip conical carbon fibre electrode that then contacts the cell cytoplasm through which the vesicles diffuse. The vesicles adsorb and stochastically rupture on the electrode surface, which is maintained at a potential positive of the neurotransmitter redox waves. Once more, oxidation of the neurotransmitters is observed as current transients, the integration of which affords the total number of molecules inside each individual vesicle.

Super-resolution microscopy. Complementary to electrochemistry are super-resolution microscopy techniques, research that culminated in the Nobel Prize in Chemistry in 2014. These are methods that avoid the diffraction limit associated with confocal microscopy. Such sub-diffraction-limit lateral resolution is made possible by interrogating fluorophores tagged to the molecules of interest. Super-resolution microscopy techniques have been used for imaging different proteins in synaptic vesicles, as well as tracking vesicle recycling (the process in which vesicles retrieve their components after exocytosis for reuse in continuous neurotransmission) using new fluorescence probes that offer molecular specificity and spatial resolution of single molecules. We briefly describe two important super-resolution methods that are being increasingly applied to understanding molecular processes in living cells[9].

Stimulated emission depletion (STED) microscopy, applied in the context of neuroscience, involves localizing fluorescent biomolecules at the synapse and synaptic vesicles. The region of interest is probed with two laser beams, one for excitation and one for stimulated emission depletion. Fluorophores that are irradiated by the doughnut-shaped depletion beam are 'turned off', whereas those in the centre of the doughnut escape this effect and only encounter the excitation beam. The result is an emission from a point smaller than the diffraction limit; interrogating an array of points affords images with high spatial resolutions on the order of ~30–40 nm.

Stochastic optical reconstruction microscopy (STORM) is similarly useful in the study of synaptic vesicles containing fluorescent molecules that are stochastically activated for emission. As a result, the positions of a subset of the fluorophores can be determined. The fluorophores used in STORM experiments must be relatively photostable because they need to be activated or switched over the course of many imaging cycles.

© 2017 Macmillan Publishers Limited, part of Springer Nature. All rights reserved.

Owing to the randomness of activation, simultaneous excitation of multiple fluorophores that are within the diffraction limit is unlikely. Thus, collecting data over hundreds to thousands of cycles can afford a final image with a resolution as low as ~10 nm.

Mass spectrometry. As with super-resolution microscopy, secondary ion mass spectrometry (SIMS) can be used for molecular imaging with high spatial resolution. Additionally, many SIMS experiments do not require the introduction of labelled molecules, providing non-targeted detection with high chemical specificity. One of the most recently developed SIMS instruments for nanoscale applications (nanoscale secondary ion mass spectrometry or nanoSIMS) enables imaging of stable isotopic species at spatial resolutions of ~50 nm, such that the molecular structure of synaptic vesicles can be readily discerned. NanoSIMS involves bombarding a surface with a highly energetic primary ion source, a process that typically does not give rise to intact secondary ions from the sample, but rather a distribution of smaller fragments. Obtaining reliable information about the molecular distribution present in the living system thus requires labelling of specific sites. When stable isotopologues of biomolecules are used, individual synapses and vesicles can be imaged and the molecular turnover can be quantified, at least on a relative scale. In this method, the region of interest is sputtered, spot by spot, with a caesium or oxygen primary ion beam, and the resultant secondary ions are then separated in a magnetic sector analyser according to their mass-to-charge ratio (m/z). Up to seven different labelled ions of interest are then detected in parallel. A key aspect of this method is the use of coaxial ion optics, which allows both the beam source and the secondary ion collector to be extremely close to the sample, leading to spatial resolutions down to ~50 nm.

Having described the principles of the analytical methods that are most useful in the study of synaptic vesicles, the remainder of this Review further explores cellular electrochemistry, as well as super-resolution optical and mass spectrometric imaging, and how these techniques are used to elucidate the structure and function of synaptic vesicles.

In vivo amperometry of neurotransmitters

Vesicles can contain a range of molecules and ions, including redox-active neurotransmitters such as dopamine, adrenaline, noradrenaline, serotonin and histamine. Each vesicular unit is small, so although the concentration of neurotransmitters in each is relatively high, only femto- to zeptomoles of the molecules are released during each exocytosis event. Because these events occur on a timescale of hundreds of microseconds to milliseconds, it is important to use techniques that are not only very sensitive, but that also have high temporal resolution[6,10–16].

Techniques for measuring exocytosis. Major developments in analytical methodology have made it possible to probe vesicle fusion and neurotransmitter release in single live cells. A range of methods allow monitoring of the location and time course of exocytosis events by quantitative means. These analytical techniques — which include fluorescence spectroscopy, electron microscopy, electrophysiology and electrochemistry — each probe the release process in a rather different way. They each afford different pieces of information, from the identities and concentrations of the molecules released to the movement of the membrane. Fluorescence imaging generally makes use of intravesicular dyes, and electrophysiology measures membrane capacitance. This latter technique is called patch clamp and involves using a small pipette tip to measure the cell membrane capacitance to quantify changes in the cell surface during exocytosis of a vesicle. These dynamic processes are less amenable for electron microscopy, which is more suited to providing high-resolution static snapshots of fixed or frozen tissue. As we have noted, electrochemistry — amperometry, to be more specific — allows for anodic currents to be measured, the magnitudes of which are proportional to the amounts of transmitter released. In comparing the techniques discussed here, one must consider that the temporal resolution of each is very different, and only fluorescence and amperometry follow the chemistry occurring during the signalling event. The temporal resolution of fluorescence spectroscopy, however, is typically about 100 ms, such that the method probably only measures slower exocytosis events during which the vesicle fully distends. Similarly, low temporal resolution is also a weakness of patch clamp methods, because the low sensitivity of these methods means that significant durations are required for sufficient data to be collected. By contrast, amperometry is much faster and more sensitive, such that smaller, faster events can be monitored. Indeed, the release process can be followed over time rather than obtaining a picture of only the final state when all of the neurotransmitters are released[17]. Thus, it is no surprise that electrochemical techniques are the dominant means to quantify chemical release during exocytosis.

In vivo amperometry. Introduced in the 1990s by Wightman and co-workers, amperometry using carbon fibre electrodes has been particularly useful (FIG. 1a). The method was initially developed as a highly sensitive and responsive means to monitor the release of chemicals from single vesicles at bovine adrenal chromaffin cells[6,17]. The charge associated with each transient allows quantification of the analyte, and the shape of the signal can be used determine the exocytosis mechanism. The rise time of the transient is thought to correspond to the opening of the fusion pore, and the half width of the spike is related to the duration of the release. An interesting aspect of many transients is the presence of a pre-spike current increase (or 'foot') assigned to the oxidation of molecules diffusing out of the initial opening of the vesicular fusion pore. Many believe this to be important in exocytosis communication and seek to discern the dynamics and stability of fusion pore opening before vesicle dilation[18–20]. Amperometry has been used to study *in vivo* exocytosis at many cell types, including

© 2017 Macmillan Publishers Limited, part of Springer Nature. All rights reserved.

primary cultures, immortalized cell lines and nerve cells. In aqueous solution, potentials of up to +1–1.4 V versus Ag/AgCl can be applied before background oxidation becomes an overwhelming issue. As a consequence, the method is limited to molecules with accessible redox waves, such as the neurotransmitters dopamine, serotonin, adrenaline, noradrenaline and histamine.

Different modes of exocytosis. Until recently, all exocytosis events observed with amperometry were thought to be mainly 'all-or-nothing' processes. The fusion event between the secretory vesicle and the plasma membrane was considered a process in which all the chemical content was released and the vesicle membrane fully distended into the cell membrane. In this way, regulation of exocytosis was based solely on the initiation of the events, studies of which were recognized with the Nobel Prize in Physiology and Medicine in 2013. Since 2010, a combination of chemical methods, including amperometry, VIEC (a new method), as well as dynamic modelling[8,21–24], have indicated that other modes of exocytosis can occur (FIG. 1b). Rather than this 'all-or-nothing' full release process, it turns out that vesicles can have their fusion pore close again before all the contents leave, a situation that may not be clear from the amperometric trace. Such a partial release exocytosis mode — whereby the vesicle opens to release a large fraction of its contents and closes again to end each exocytosis event — appears to occur more frequently than full release[21]. Distinct from partial release exocytosis is a third process — 'kiss-and-run exocytosis' — in which the vesicle and cell membrane form an initial fusion pore that rapidly closes. The time over which the pore is present is very short, and only a very small fraction of the neurotransmitter is released (a similar concentration is released in the pre-spike foot during normal exocytosis events discussed above) in small, fast amperometric events (known as flickering)[25,26].

Observation of a post-foot[27] is consistent with the partial opening of vesicles during exocytosis. In this case, the post-foot signal corresponds to the molecules being continually released through the fusion pore as it narrows and closes. It has been suggested that the fluorescence and patch clamp methods discussed above only measure full release events, with amperometry mostly measuring partial release events, which are apparently more frequent[5,21]. The molecular interactions that trigger exocytosis are of great interest, and it has been proposed that vesicles and membranes feature soluble *N*-ethylmaleimide-sensitive factor attachment protein receptor (SNARE) proteins that recognize each other and allow the vesicle and membrane to dock and fuse[28]. Central to the SNARE hypothesis are the proteins, which directly regulate the frequency of exocytosis events. The recent discovery of partial release events opens a new paradigm in neuronal regulation, because apparently it is the closing of a vesicle, rather than its opening, that is key to regulating individual events and synaptic strength.

Quantifying transmitter release at single nerve cell varicosities and synapses. The fruit fly, *Drosophila melanogaster*, is a popular model organism for the study of complex biological processes related to the nervous system using both molecular and genetic approaches. The nervous system of *D. melanogaster* is relatively simple, but it still has many of the same higher-order brain functions observed in mammalian brains. Studying the nervous system of fruit flies can thus provide information relevant to several human neurodegenerative diseases, such as Alzheimer disease, Parkinson disease and Amyotrophic lateral sclerosis[29–31]. Live, dissected *D. melanogaster* larvae were examined by a novel method used to study exocytosis of octopamine (4-(2-amino-1-hydroxyethyl)phenol) from small varicosities — bulbous regions along axons in the neuron that appear to act like open synapses[32] (FIG. 2A). The neuromuscular junction is located at the periphery and can be readily accessed with a small-tip electrochemical probe. Additionally, the superficial position of octopaminergic neuronal boutons in the larval body wall allows electrode placement on the varicosity. Under optimized conditions, optogenetic stimulation induces release of octopamine, which is reproducibly detected in the form of many anodic current transients (FIG. 2B). Each transient arises from an individual release event and the simple events (those associated with a single peak) observed each involve the release of

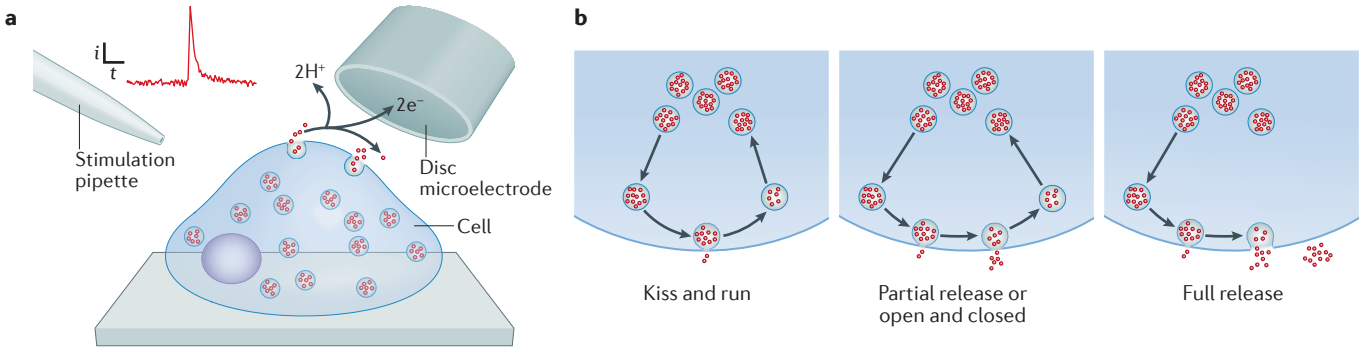

Figure 1 | **Illustration of single-cell amperometry and three modes of exocytosis. a** | Schematic illustration of exocytosis monitoring using single-cell amperometry with a disc carbon fibre microelectrode. The inset depicts a typical amperometric spike that represents an exocytosis event. **b** | Summary of different modes of exocytosis, including 'kiss and run', 'open and closed' (also referred to as partial release), and complete release with full vesicle distension.

© 2017 Macmillan Publishers Limited, part of Springer Nature. All rights reserved.

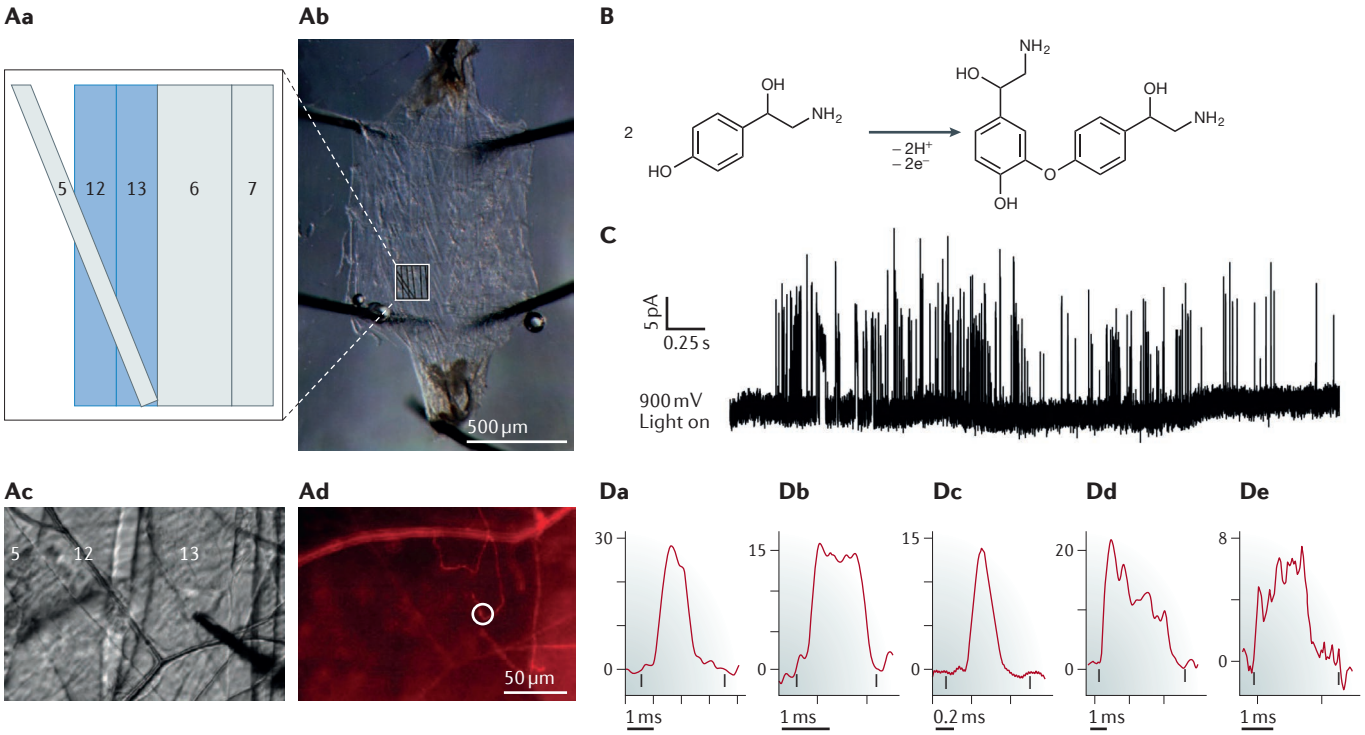

Figure 2 | **Amperometric measurement of octopamine release from a neuronal varicosity in a *Drosophila melanogaster* larva. A** | The muscle fibres and nerve terminals of the *Drosophila melanogaster* larval system. **Aa** | The muscle structure in one hemisegment of the body wall. **Ab** | A filet of the muscle wall of the 3rd instar *D. melanogaster* larvae. **Ac** | Microelectrode placement on the type II varicosities in muscle 13. **Ad** | The same view as that in panel **Ac** but with the red fluorescence protein mCherry at octopaminergic terminals (type II varicosities), which are visible as red lines (the white ring shows the location of the microelectrode). **B** | Electrochemical oxidation and coupling of two octopamine molecules. **C** | Example of amperometric measurement of octopamine release from single traces collected at a microelectrode on the type II varicosities in muscle 13 of *D. melanogaster* muscle neurons labelled with mCherry. A carbon fibre microelectrode 5 µm in diameter was used for the experiment, with an electrode potential of 900 mV (versus Ag/AgCl reference). Exocytosis was triggered by blue light stimulation. **D** | Different exocytosis events give rise to different electrochemical responses. **Da** | Two overlapping current peaks. **Db** | A plateau complex event. **Dc** | A single event. **Dd** | A complex event with decreasing current during the event. **De** | A complex event with increasing current. Panels **A**–**C** are reproduced and panel **D** is adapted with permission from REF. 32, Wiley-VCH.

~22,000 molecules (FIG. 2C). Moreover, different types of release give rise to current transients with different shapes (FIG. 2D), and, as noted above, this is related to the mechanism by which the vesicle opens to make a nanometre-wide fusion pore. It has been speculated that partial release involves the pore opening just the right amount to release the necessary fraction of neurotransmitter at the necessary rate. This further suggests that the partial release of transmitter is important in regulating transmission, and there may be further mechanisms with plasticity in the rate and fraction released.

A long-standing challenge in the chemical quantification of neurotransmitter release has been to place a nanoelectrode in the synapse between two communicating cells. This challenge has been met with nanotip electrodes[33,34], which are fabricated by flame etching carbon fibres sealed with epoxy in glass micropipettes. The response of these nanotip electrodes can be characterized voltammetrically[34,35]. When ready, electrodes can be placed in the synapses of superior cervical ganglion cells in culture to monitor release of the neurotransmitter noradrenaline (FIG. 3).

The synaptic space between cells is very small (~20 nm), such that microscopy and chemical techniques are required to accurately locate the nanotip. To ensure the electrode was placed in the synapse, the solution was spiked with $[Ru(NH_3)_6]^{2+}$, a redox-active complex that does not penetrate the cell membrane. As the electrode is inserted into the synapse, less current assigned to the oxidation of $[Ru(NH_3)_6]^{2+}$ is observed, consistent with the electrode being in a location less accessible to the complex. Spiking the K^+ concentration elicits exocytosis, with the release of the readily oxidized noradrenaline molecules being observed as current transients detected by the nanotip electrode. These events are extremely fast (<1 ms, FIG. 4), and close examination of individual events suggests possible flickering of the pore upon vesicle contact, resulting in the development of a small opening through which some contents escape the cell membrane.

The results of the experiments in live fly neurons and the neuromuscular junction, when considered with the aforementioned observation that most exocytosis events are partial[5,21], have revolutionized the way in which we think about exocytosis. Indeed, it occurs to a partial

© 2017 Macmillan Publishers Limited, part of Springer Nature. All rights reserved.

extent, such that cells can regulate individual events and effect complex signalling. The signalling within the brain is, at its most basic event level, not purely digital (as would be the case with all-or-nothing signalling) but is best considered as an analogue or perhaps modified digital process.

Intracellular VIEC of single vesicles

Cells expel transmitters at variable amounts and with variable dynamics that depend on stimulation by other chemicals[36–43]. This raises questions about how much of a transmitter is initially stored in vesicles and the factors controlling the fraction of transmitter that is released during exocytosis. Answering these questions and understanding neuronal transmission requires a method for quantifying transmitter concentrations in single vesicles.

Vesicle impact electrochemical cytometry. The first successful attempts at measuring vesicle content led to the development of a method termed flow electrochemical cytometry. This approach uses a microfluidic chip that separates vesicles by capillary electrophoresis before exposing them to a sheath-flow of sodium dodecyl sulfate, a surfactant that breaks the vesicle membrane to release electroactive transmitters that can be detected by a microelectrode[8,44,45]. Made of carbon fibre, the microelectrode oxidizes the molecules to allow their quantification in each vesicle. This method has been used to measure transmitter content in single artificial vesicles (liposomes) and vesicles isolated from cell lines or brain tissue. At present, the complexity of the instrumental setup, which involves alignment of a small electrode in the stream flowing from the capillary, seriously limits the applications and widespread adoption of this method.

VIEC represents a new and simpler technique that allows mammalian vesicles to adsorb and stochastically rupture on a carbon electrode that oxidizes transmitters[23,46]. This procedure, which eliminates the need for separation or addition of lysis buffer, allows convenient detection of the transmitters expelled from single vesicles. Integration of the resulting single current transients enables quantification of the molecule of interest. Many transients can be detected either directly in a vesicle suspension or following pretreatment of the electrode in a concentrated vesicle suspension and transfer to a vesicle-free buffer solution. Experiments using a quartz crystal microbalance with dissipation and scanning electron microscopy (SEM) have been used to show that vesicles adsorb and stay on the electrode before application of potential[24], supporting the theory that mammalian vesicles adsorb and subsequently rupture on the electrode in VIEC. The amount of catecholamine detected by VIEC allows calculation of vesicle size, with the resulting figures being in agreement with independent data from nanosight tracking analysis[23], such that the efficacy of VIEC for the quantification of transmitter storage in single vesicles is validated.

In an electrochemical context, the potential applied to oxidize catecholamine at the working electrode is usually +700 mV relative to a Ag/AgCl reference. SEM imaging suggests that the vesicles become adsorbed on the electrode surface, resulting in a strong electric field across the 5 nm-thick vesicle membrane. Assuming there is no gap between the membrane and the electrode surface, the electric field across the membrane is on the order of 10^6 V cm^{-1}, a typical value required for electroporation of membranes. For VIEC experiments, potentials of +500 and +900 mV have also been used, with an increase in the event frequency observed as the potential increases. This indicates that electroporation is at least one of the forces driving the opening of the vesicle membrane and the expulsion of vesicular catecholamine to the electrode[47].

It has been noted that protein-free liposomes are 20 times more likely to rupture on the electrode than mammalian vesicles[47]. This has led to speculation that vesicle membrane proteins protrude, creating a small gap between the electrode and lipid membrane that might limit electroporation and decrease the frequency of vesicle rupture, as evidenced by VIEC measurements[47]. The proteins in contact with the electrode apparently need to diffuse or migrate away to allow the lipid membrane to be close enough to the electrode for electroporation to occur. Further information regarding the regulatory role of membrane proteins in vesicle rupture during VIEC comes from studies comparing peptide-decorated liposomes with protein-free liposomes,

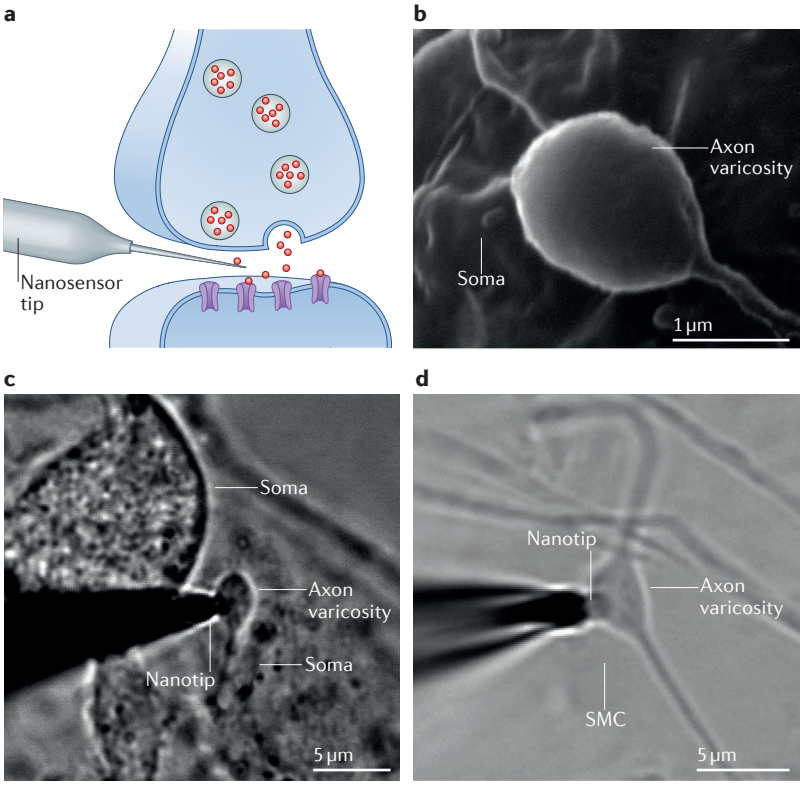

Figure 3 | **Amperometric measurement of noradrenaline release from single cultured neurons. a** | Schematic illustration of a nanosensor tip (~100 nm) inside a synapse. **b** | Scanning electron microscope image of a synapse formed between cultured superior cervical ganglion (SCG) sympathetic neurons. **c** | A bright-field photomicrograph of the nanosensor tip inside a synapse, between a varicosity of one SCG neuron and the cell body of another. **d** | A photomicrograph of the nanotip inside a synapse, between a varicosity of a SCG neuron and a smooth muscle cell (SMC). Figure is reproduced with permission from REF. 34, Wiley-VCH.

© 2017 Macmillan Publishers Limited, part of Springer Nature. All rights reserved.

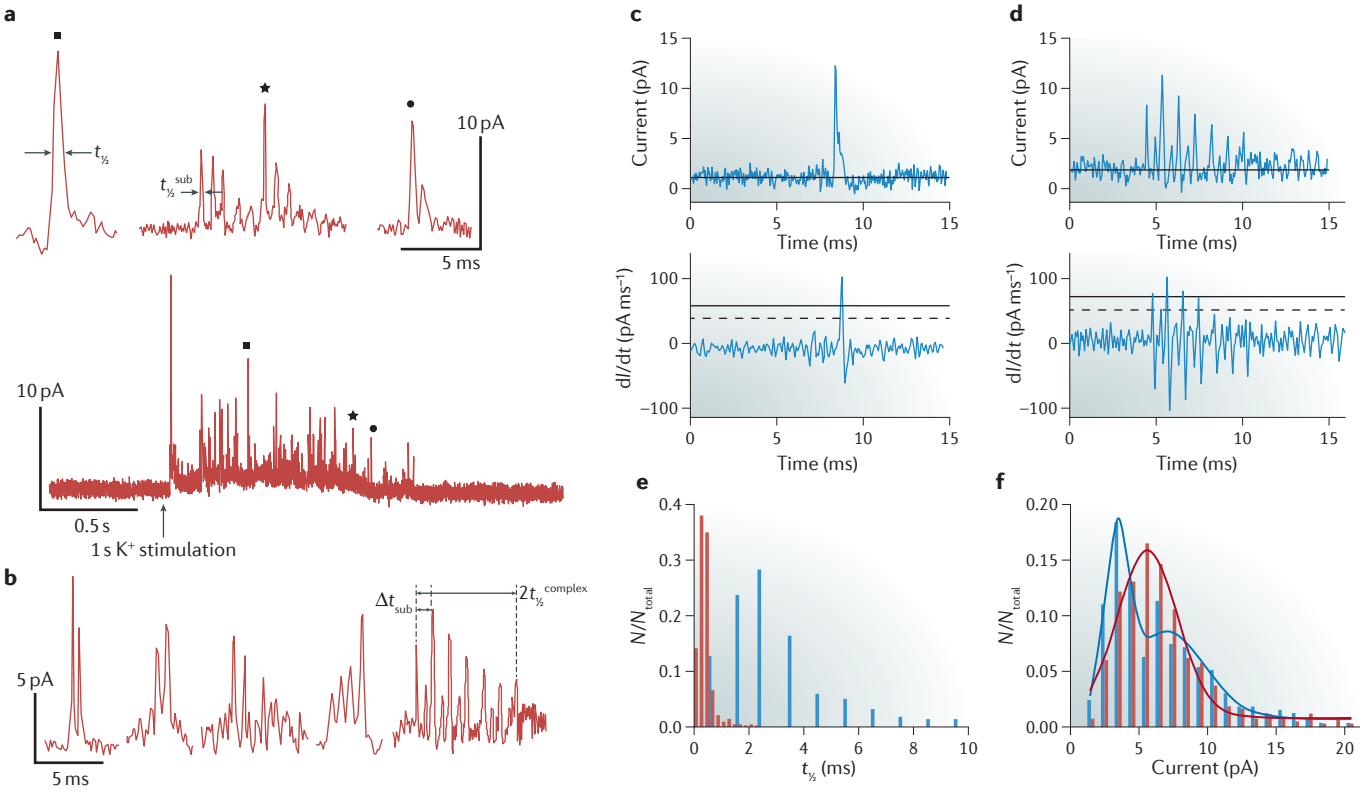

Figure 4 | **Nanoelectrode amperometry allows monitoring of vesicular exocytosis inside a synapse between SCG neurons. a** | A K^+-induced amperometric spike is followed by two complex events (expanded view of events are shown above the overall current trace). **b** | Representative examples provide a timescale over which such complex events typically occur. **c**,**d** | Amperometric current transients (top) and their first derivatives (dI/dt, bottom). Panel **c** depicts a simple transient and panel **d** a complex one. The solid and dotted lines are 3 × RMSE and 5 × RMSE, respectively. **e**,**f** | Histograms of simple (red) versus complex (blue) event characteristics in $t_{1/2}$ ($n = 400$ for simple events and $n = 532$ for complex events) and peak height (I_{max}; $n = 433$ for simple events and $n = 544$ for complex events). The *y* axis corresponds to the fraction of neurotransmitter released — the quotient of neurotransmitter released (*N*) to the total content in the vesicle (N_{total}). RMSE, root-mean-square error; SCG, superior cervical ganglion. Figure is reproduced with permission from REF. 34, Wiley-VCH.

as well as with mammalian vesicles isolated from adrenal glands[47]. Amperometric measurements of stearoyl octaarginine-decorated liposomes suggest that their vesicles open more slowly than those in protein-free liposomes but much faster than those in mammalian vesicles. These results indicate that peptides or proteins in the membrane modulate vesicle opening in VIEC by restricting pore opening during electroporation and slowing vesicle rupture. Experiments of the present type might eventually help us to understand how membranes interact during membrane–membrane fusion.

An amperometric transient typically decays exponentially, reflecting neurotransmitter diffusion from the interior of the vesicle to the electrode surface. The rate of decay is used to estimate the size of the pore formed at the membrane using VIEC. As expected, peptide-decorated liposomes display smaller pores than clean liposomes, consistent with the assumption that proteins retard pore opening in electroporation. The interiors of soft nanoparticles, such as protein-free and peptide-decorated liposomes, do not feature dense cores, and the flow of small molecules (such as catecholamines) from the interior towards the electrode is simply a diffusion-controlled process. However, the sizes of the pores formed by chromaffin vesicles are considerably larger[47]. This apparently results from slower diffusion of catecholamine from the constrained protein matrix (dense core) of chromaffin vesicles, thus causing the pore to expand over a longer time period. This is different from exocytosis, in which some proteins, such as actin, appear to restrict expansion of the pore[48].

The mechanism by which vesicles rupture at the electrode surface in VIEC can be further probed by monitoring the release of fluorophores such as rhodamine and nitrobenzoxadiazol (NBD)[49]. For example, rhodamine-tagged phosphatidylethanolamine molecules can diffuse into a vesicle membrane upon incubation. Excitation of the rhodamine moieties ($\lambda_{ex} = 550$ nm) in the membrane significantly enhances the rupture of vesicles on electrodes, leading to a 20-fold increase in the number of amperometric spikes relative to control experiments in which either the dye or light are not present. The effect of excited rhodamine on vesicle opening is dependent on the amount of rhodamine inserted and the excitation power used. Another dye, nitrobenzoxadiazol-phosphoethanolamine (NBD-PE), also leads to similar

© 2017 Macmillan Publishers Limited, part of Springer Nature. All rights reserved.

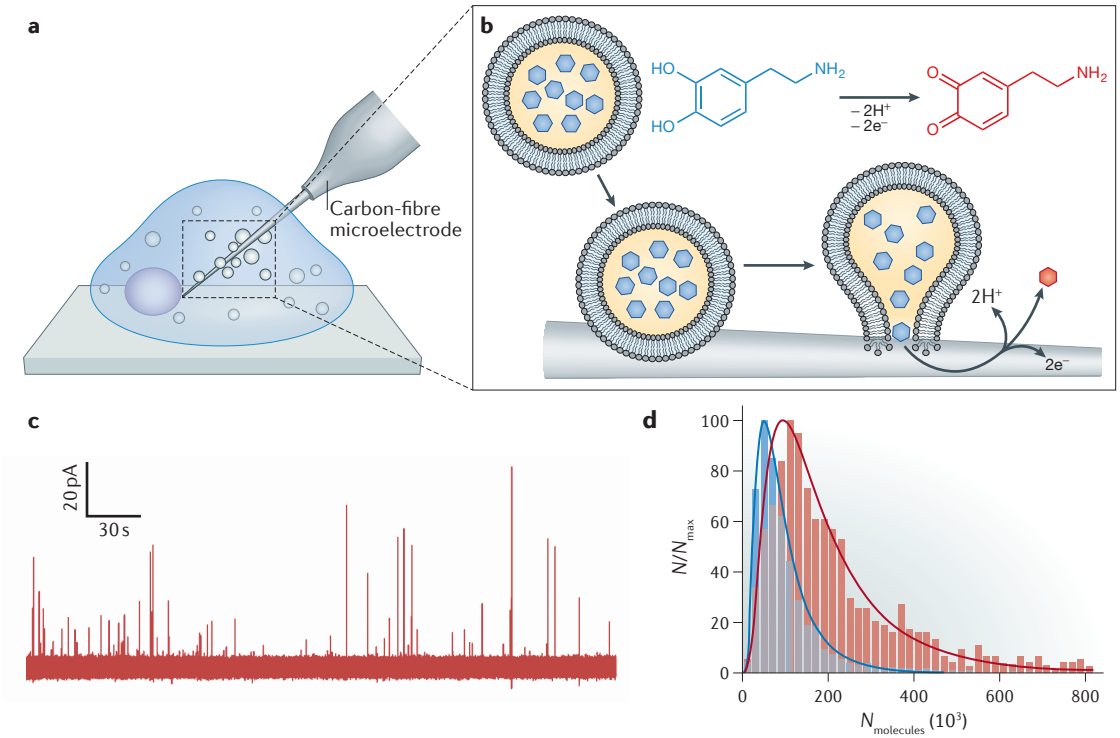

Figure 5 | **Intracellular VIEC allows quantification of vesicular transmitter content in live cells. a** | Schematic illustration of a nanometre tip conical carbon-fibre microelectrode placed in the cytoplasm of a single rat pheochromocytoma PC12 cell. **b** | Dopamine released from a vesicle can undergo two-electron oxidation to dopamine quinone at the *in situ* microelectrode. **c** | Amperometric traces for a nanometre tip conical carbon-fibre microelectrode placed inside a PC12 cell. **d** | Normalized frequency histograms describing the distribution of vesicular catecholamine as quantified in untreated control PC12 cells using intracellular VIEC (red, $n = 1{,}017$ events from 17 cells) and by K^+-stimulated exocytosis at the same electrode by single-cell amperometry (blue, $n = 1{,}128$ events from 17 cells). The bin size is 2×10^4 molecules. The data were fit to a log normal distribution. VIEC, vesicle impact electrochemical cytometry. Panel **a** is adapted and panels **c** and **d** are reproduced with permission from REF. 24, Wiley-VCH.

enhancement of vesicle rupture, albeit at a shorter excitation wavelength (460 nm). The precise structure of the fluorophore — namely, the position of fluorophore in the fluorophore-PE compound — affects the pore opening process over a different timescale. When NBD is attached to the head group of PE, the fluorophore ends up outside the lipid membrane. Excitation of the NBD groups gives rise to a peak enhancement (~35 times) in the number of VIEC events, but only after a delay of approximately 400 s after irradiation begins. If NBD is instead attached to the lipid chain of PE, only a tenfold enhancement is observed, although it begins immediately and persists for the entire detection period (0–600 s). The long delay time observed when NBD is placed at the PE head group suggests that the enhancement of vesicle rupture following excitation of the fluorophore is not merely a simple energy transfer process that induces electroporation. This enhancement might instead result from the excited dye generating reactive oxygen species (ROS) that oxidize the membrane lipids (or proteins). This process could lead to water defects and changes in the properties of the membrane, which would become thinner and come into closer contact with the electrode. Such effects would be more pronounced for a reaction inside the membrane than outside it, resulting in greater ease of electroporation, more rapid onset and higher frequency of events. The occurrence of water defects and membrane thinning can also be triggered by dimethyl sulfoxide (DMSO), which leads to similar effects on vesicle rupture in VIEC[49]. Further, under certain conditions, VIEC experiments can show that liposomes adsorb on platinum nanoelectrodes but do not rupture immediately[50]. However, rupturing does occur when the polyethylene glycol (PEG)-based surfactant Triton X-100 is present, with a mechanism that is probably similar to that occurring in the fluorophore and DMSO examples described above. Overall, changes in the vesicular lipid double-layer membrane, the main participant in electroporation, influence the occurrence of current transients in VIEC.

Two mechanisms have been suggested for vesicle opening in VIEC, and in both of these the vesicles diffuse to the electrode, are adsorbed and subsequently rupture to release the transmitter, which is oxidized quantitatively at the electrode[46,47]. In one model proposed by Compton and co-workers[46,51], the vesicle ruptures and fully collapses, whereas in another model, proposed by us, the vesicle opens to form a pore at the point of contact with the electrode — a process driven by electroporation[47]. The pore created allows the content of the vesicle to diffuse to the electrode for subsequent electrochemical quantification. The rupturing of vesicles on

© 2017 Macmillan Publishers Limited, part of Springer Nature. All rights reserved.

the electrode is affected by the applied potential, the membrane protein, protein dense core, the presence of ROSs and the membrane thickness. Other factors, such as temperature, vesicle size and membrane lipid tension, might also influence vesicle opening and thereby impact VIEC. The full collapse scenario is not consistent with all of the observations reported thus far, but the data from Compton and co-workers are consistent with the electroporation mechanism. The actual mechanism remains an open question.

Development and applications of intracellular VIEC. The intracellular version of VIEC is a recent adaptation that has enabled the measurement of transmitter content in single vesicles in the cytoplasm of live cells[24] (FIG. 5). A nanometre tip conical carbon fibre electrode, fabricated by flame-etching, is used to penetrate the cell membrane and expose the electrode surface to cellular vesicles. These then adsorb and subsequently rupture, allowing their contents to be oxidized and quantified in a process carried out in the live cell (FIG. 5a,b). A series of well-defined amperometric transients is observed (FIG. 5c), the integration of which allows transmitter quantification. The vesicle contents are the same as those observed in vesicles isolated from identical cells, and models of vesicle opening show that the pore opening during VIEC is smaller than the electrochemical nanotip[47]. Therefore, 100% of the content in the vesicles is detected in intracellular VIEC. With this method, the mean amount of transmitter in each vesicle can be compared by monitoring the amount of transmitter released during exocytosis in a sequential experiment with the same electrode placed on a neighbouring cell. The intracellular VIEC-derived distribution of vesicular catecholamine content can then be compared with the molecular distribution obtained when K^+-stimulated exocytosis is studied using single-cell amperometry (FIG. 5d). On average, about 64% of the catecholamine molecules stored in a vesicle are released during exocytosis. Once more, we see the prevalence of partial exocytosis processes, in which the vesicle must close again to prevent all the content from coming out.

L-3,4-Dihydroxyphenylalanine (L-DOPA) is the direct biochemical precursor to catecholamines in mammalian cells. This precursor is the main drug in the clinical treatment of Parkinson disease and dopamine-responsive dystonia. Intracellular VIEC has been used to show that L-DOPA treatment increases the amount of dopamine released during exocytosis from pheochromocytoma (PC12) cells[24]. Interestingly, the fraction of transmitters released from L-DOPA-treated PC12 cells is the same as that from control cells. Thus, this drug increases both the dopamine initially in the vesicles as well as that released during exocytosis.

Intracellular VIEC has also been used to study side effects of chemotherapy, particularly the so called chemo brain, a cognitive deficiency in many patients with cancer. This deficiency, thought to be related to the exocytosis process, was studied at the single-cell level with a combination of single-cell amperometry and intracellular VIEC[52]. Cisplatin (*cis*-$[PtCl_2(NH_3)_2]$), the first clinical platinum-based anticancer drug, does not significantly influence transmitter storage in PC12 cell vesicles after 3 hours of incubation. However, the amount of transmitter released during single exocytosis events does change depending on the cisplatin dosage. At low doses of cisplatin (1–5 μM), each cell gives rise to more exocytosis events, which are, on average, of a short duration. However, at high concentrations of cisplatin (10–100 μM), the opposite effect on exocytosis dynamics is observed — the events are less frequent but longer, such that each event leads to a larger fraction of the vesicle content being expelled. The mechanism by which cisplatin modulates exocytosis is not through any alteration of vesicle properties but rather from a change in the cell membrane (lipid and/or protein).

The combination of intracellular VIEC and single-cell amperometry provides a powerful approach to study vesicle properties and transmitter release during exocytosis. Recently, this approach has been used to investigate the effects of Zn^{2+} ions on exocytosis[53]. Zinc(II) is thought to regulate learning in mammals and, as shown by these electrochemical methods, regulates the fraction of transmitter released during exocytosis as well as the dynamics of the process. It can therefore be assumed that these exocytosis parameters are important in learning and memory. Intracellular VIEC and amperometry are also useful in studying biophysical aspects of cellular exocytosis. In 2000, Colliver *et al.*[54] discovered that transmitter vesicles grew and shrank with transmitter load, with the internal concentration remaining constant. These measurements were based on contents released; however, they are valid because the treatments that were used (L-DOPA and reserpine) affect vesicle content and release to the same extent. Fathali and co-workers[55] have recently applied intracellular VIEC and amperometry experiments in combination with electron microscopy to show that extracellular osmotic stress reduces the vesicle size and amount released during exocytosis, but does not affect the neurotransmitter concentration in the vesicle. The concentrations could be determined by dividing vesicle content (measured by intracellular VIEC) by the volume (determined by electron microscopy). It is noted that the authors of this study did not correct for plane of section in the electron microscopy of the vesicles.

Structure and activity of synaptic vesicles

Super-resolution microscopy (STED and STORM). Research in neurobiology, molecular and cell biology has made great use of optical microscopy to explore subcellular architectures and the dynamics of cellular macrobiomolecules. Compared with electron microscopy (another major imaging technique in cell biology), optical microscopy is advantageous in that it can allow visualization of specific biomolecules and imaging of living cells. Immunocytochemistry can make use of fluorophore-tagged antibodies, whereas visualization of many subcellular networks and the dynamics of cellular processes use genetically encoded green fluorescent protein (GFP) labelling. The diffraction of light limits the spatial resolution of fluorescence microscopy to $\lambda/2$, with the best available aperture affording ~200 nm

© 2017 Macmillan Publishers Limited, part of Springer Nature. All rights reserved.

lateral and ~500 nm axial resolution[56]. Evidently, such a method cannot resolve many subcellular structures and organelles, such as the presynaptic and postsynaptic structures, as well as the vesicles of importance to neurobiology. To overcome the resolution limit inherent to fluorescence microscopy, the technique has spawned several specialized technologies that have been increasingly embraced in the biological and chemical communities. We refer here to near-field scanning optical microscopy, total internal reflection fluorescence microscopy, structured illumination microscopy, stimulated emission depletion (STED) and stochastic optical reconstruction microscopy (STORM)[9,56]. Although each method has its own advantages and limitations and is suitable for specific biological applications, the last two have been of particular utility in neuroscience and cell biology, especially in the field of synaptic research.

First developed and demonstrated by Hell and Wichmann[57] in 1994, STED has since been further expanded to allow for one- and two-photon excitations and live imaging approaches[58,59]. In principle, the technique requires two laser beams, one for excitation and the other for stimulated depletion of fluorescence emission of fluorophores (FIG. 6a). The doughnut-shaped depletion beam is superimposed on the excitation beam, which 'turns off' the emission of the fluorophores in the depletion beam due to stimulated emission. This results in an excited fluorophore relaxing to the ground state without fluorescence upon absorbing a photon, the energy of which is equal to the energy difference between the ground and excited state of the fluorophore. Thus, the fluorescence emission occurs only at the centre where the intensity of the depletion beam is zero. The depletion beam can therefore reduce the size of the fluorescing spot to a size that is smaller than the diffraction limit. The image is assembled by scanning either the laser beam or the sample spot-by-spot or pixel-by-pixel. Similar to confocal microscopy, STED makes use of a pinhole to remove out-of-focus light. Several conditions must be satisfied to obtain the best STED images. The fluorophores should be non-toxic to living cells, highly selective for specific proteins, easily depleted with a low energy depletion beam and sufficiently photostable[60]. In addition, the choice of the excitation and depletion beam depends on the excitation and emission wavelength of the fluorophores. In particular, the excitation wavelength must match that of the fluorophores to obtain the highest possible fluorescence intensity, whereas the depletion wavelength must be different from the excitation and the emission bands of the fluorophores. The doughnut shape of the depletion beam is obtained using a phase mask, which might take the form of a spiral spatial phase modulation or vortex phase plates[61,62]. The zero intensity at the centre of the depletion beam is crucial in achieving the ultrahigh spatial resolution with this technique, which is on the order of ~30–40 nm laterally and ~500 nm axially[56,60]. The axial resolution (in the *z* direction) is no better than that from conventional fluorescence microscopy unless a second depletion beam is installed in this direction[63], or unless the combination of STED with a modified version of STED (4Pi imaging) is applied[64].

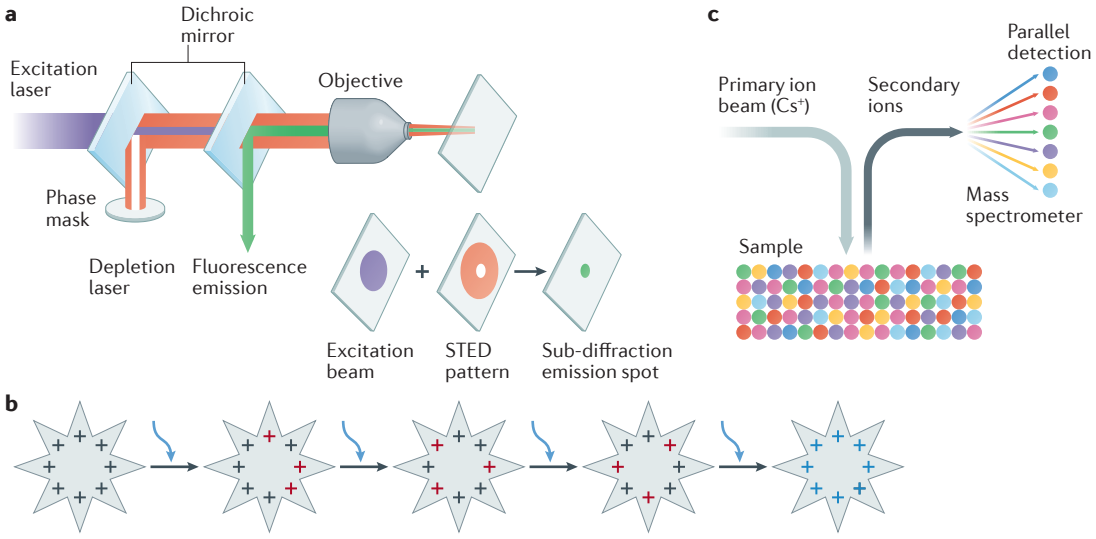

Figure 6 | **Principles of super-resolution STED, STORM and nanoSIMS imaging. a** | STED uses superimposed excitation and depletion laser beams, the latter having zero intensity at the centre after passing through a phase mask. Thus, emission depletion of fluorophores does not occur at the beam centre, which is the emission point from which sub-diffraction resolution is possible. **b** | STORM makes use of photoswitchable fluorophores that are switched on and off through many cycles. Only a subset of fluorophores is activated in each cycle, and the final image is constructed from all fluorophore positions obtained from hundreds or thousands of cycles. **c** | NanoSIMS samples incorporate stable isotopic labels into their structures. Analysis involves a primary Cs^+ ion beam sputtering the sample surface spot-by-spot. As a result, secondary ions are ejected from the surface and are separated according to their mass-to-charge ratio (ions at up to seven different *m*/*z* values can be detected in parallel). The coaxial nature of the primary and secondary ion paths helps to increase spatial resolution. SIMS, secondary ion mass spectrometry; STED, stimulated emission depletion; STORM, stochastic optical reconstruction microscopy.

© 2017 Macmillan Publishers Limited, part of Springer Nature. All rights reserved.

A technique similar to but distinct from STED is STORM, which can be used to determine the position of a subset of stochastically activated fluorophores (FIG. 6b). When the distance between two fluorophores is smaller than the diffraction limit of visible light (~200 nm), it is impossible to resolve the two points of fluorescence using conventional microscopy. However, if the fluorophores emit at different timepoints, their positions can be sequentially and accurately observed by temporal discrimination. Photoactivatable and photoswitchable fluorescence dyes or proteins are densely distributed throughout the region of interest and are imaged over many cycles. This principle is the basis for STORM and other similar techniques such as photoactivated localization microscopy (PALM)[65,66]. Owing to the random nature of activation, the probability of two fluorescing molecules being within ~200 nm of each other is negligible. Indeed, in most cases, the positions and intensities of single fluorophores can be archived. The final image is then constructed from hundreds or thousands of individual measurements from all the cycles. The resolution of the technique is related to the precision with which the fluorophore can be located, which, in turn, depends on the number of photons detected from each fluorophore per cycle. STORM can allow imaging with ~10 nm lateral and ~20 nm axial resolution[67]. Importantly, the fluorophores used in STORM must be bright and photostable because they are typically turned on and off through hundreds or thousands of photoactivation cycles. The wavelength of light used for photoactivation must not coincide with either the excitation or the emission bands of the fluorophores. Common photoswitchable fluorophores used in STORM include cyanine dye, cyan/dark-to-green fluorescence proteins, green-to-red fluorescence proteins and photochromic rhodamine[9].

Although both STED and STORM are used to determine the molecular-level structures of living systems, they do this in very different ways. First, STED relies on a laser scanning approach, whereas STORM is based on stochastic activation and localization of a subset of individual fluorophores. Second, the speed of imaging in STED is higher than STORM, making STED the preferred method for imaging dynamic biological processes in living cells or tissues. On the other hand, STORM is superior for imaging large areas in which many activated fluorophores are localized. Further, enhancing sensitivity by increasing laser intensity is more likely to cause photobleaching of the fluorophores in STED than it is in STORM. Both methods have been applied in cellular neuroscience, especially to study the molecular architecture of the synapse and vesicles and their dynamic processes, such as endocytosis, exocytosis, vesicle movement, transport and reclycling[68–71]. Efforts targeted at developing multicolour imaging, 3D imaging and imaging in live systems promise to enhance the utility of these methods[58,59,72]. These advances have been enabled by engineering of optics configurations and the introduction of new labelling probes. Finally, we note the recent introduction of MINFLUX, a technique that couples the 'best' features of both STED and STORM to enable very fast small-field imaging with excellent lateral resolution (≤6 nm)[73].

Different fluorescence labelling methods for super-resolution microscopy. The outstanding performance of super-resolution microscopy, in particular STED and STORM, for cellular imaging is in part owing to the extensive development of fluorophore labels and methods for their incorporation into biomolecules. There are several desirable properties of a labelling probe for STED and STORM. These fluorophores have to permeate into the living system, where they must be nontoxic and bind to the target molecules with high selectivity. A fluorophore should be as small as possible to not only have negligible effects on normal biological function, but also to allow for the best achievable spatial resolution. It should have high brightness for its fluorescence to be much stronger than the background and so that high contrast images can be acquired. The excitation and emission wavelengths should be accessible to the excitation and emission beams in the instrument. Photostability is an essential prerequisite, and the spontaneous conversion rate between the ground and excited states must be slower than the rate of light-controlled activation. Finally, fluorophores used in STORM must be switchable through many cycles.

Fluorescence probes for super-resolution imaging can be classified into several categories (TABLE 1). One category is affinity probes including antibodies and nanobodies. The most common labelling method for conventional fluorescence microscopy involves the use of antibodies with a total size (primary and secondary antibodies) of about 20–30 nm. As we have noted, the use of large labels or (more commonly) large labelled biomolecules can limit spatial resolution, and large antibodies might not bind to all the epitopes that are within a distance less than the size of the antibody. For example, a comparison between labelling with small molecule probe aptamers and immunostaining with antibodies on the endosomes revealed that the former method afforded higher labelling density, allowing detailed endosomal structures to be visualized[74]. This detail was not accessible with the antibodies, which additionally have a tendency to cause clustering of target proteins in live cell imaging[75]. High-resolution imaging requires a high labelling density, which is difficult to obtain with large immunolabelling probes such as antibodies. Indeed, this has motivated the development of nanobodies, small tags that are as specific as conventional antibodies but have one protein domain instead of the two protein chains in normal antibodies. Nanobodies, which are about one-fifth the size of normal antibodies, can conjugate to fluorophores for direct immunostaining. This method is also advantageous as the concentration needed with direct staining is an order of magnitude less than that necessary for indirect immunostaining, a method that requires primary plus secondary antibodies[76,77].

Ries and co-workers[76] incorporated the Alexa Fluor 647 tag into anti-tubulin nanobodies that can specifically bind tubulin in fixed Ptk2 cells. In parallel, a similar experiment using antibodies instead of nanobodies was also conducted, with super-resolution microscopy imaging used to evaluate each method. The tubulin diameter is 25 μm, with the value measured using nanobodies only

© 2017 Macmillan Publishers Limited, part of Springer Nature. All rights reserved.

differing by 10%, whereas that obtained using normal antibodies differed by 50%. In another example, nanobodies have been used in STORM imaging to locate major proteins in the human nuclear pore complex. The proteins of interest, which constitute the machinery for biomolecule transport in and out of the cell nucleus, are tagged with GFP through cell transfection and then immunolabelled with anti-GFP nanobodies. Through this methodology, remarkable super-resolution images of the nuclear protein complex can be obtained in which the component locations are known with sub-nanometre precision[78].

The use of nanobodies is a selective and robust labelling method highly compatible with super-resolution imaging. However, the applications of this method have so far been limited to nanobodies that recognize GFP, which necessitates either the expression of GFP with the protein of interest or the use of customized nanobodies that bind to specific proteins of interest. Genetically encoded probes, including fluorescence proteins and small

Table 1 | **Fluorescence labelling methods for nanoscale molecular imaging**

Probes	Properties	Mechanism of labelling	Common compounds	Refs
Nanobodies	Very small, high affinity labelling	Immunolabelling 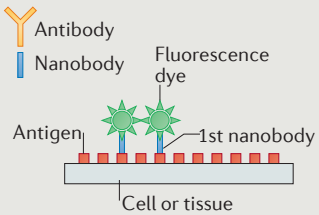	Camelid nanobodies	76,77
Small molecule fluorophores	• Small size, high brightness and photostable • Reversibly photoswitchable or photoactivatable probes are also available	Genetic fusion, enzyme mediated protein labelling, and immunolabelling 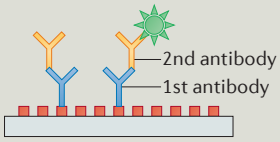	Alexa Fluor, Atto, cyanines, rhodamines and carbopyronines	9
Fluorescence proteins	Specific labelling, classified as photoshiftable, reversibly or irreversibly photoactivatable fluorescence proteins	Genetic fusion 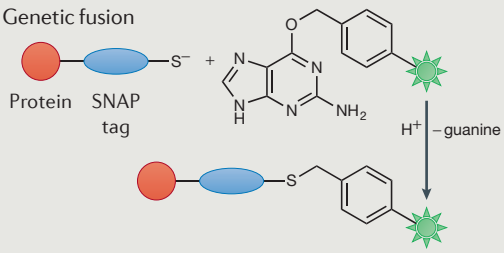	GFP, YFP, mCherry, mEos, Dronpa, Dendra and Kaede	9,97
Genetic coded labelling probes with click chemistry	• Very specific labelling of membranous proteins • Small probe can also be manipulated for multimodal imaging	Genetic expansion and click chemistry 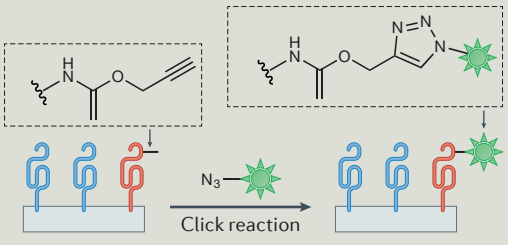	• Alexa Fluor, Star (for super-resolution microscopy) • SK155 and TriazNF1 (for multimodal super-resolution microscopy and nanoSIMS)	79,91,92
mCLING	• Label plasma membrane lipids • Efficiently fixed during immunostaining • Membrane-specific probes are internalized via endocytosis	Incubation 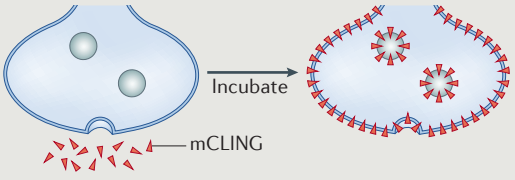	mCLING	82

GFP, green fluorescent protein; mCLING, membrane-binding fluorophore–cysteine–lysine–palmitoyl group; SIMS, secondary ion mass spectroscopy; YFP, yellow fluorescent protein.

© 2017 Macmillan Publishers Limited, part of Springer Nature. All rights reserved.

molecule probes installed using click chemistry, have also been investigated[79,80]. The growing repertoire of labelling approaches useful for super resolution also encompasses other classes of chemical probes; aptamers, the oligonucleotides selected from a sequence pool for a target protein, are known to bind to proteins specifically[74,81]. Another example is the use of the membrane-binding fluorophore–cysteine–lysine–palmitoyl group (mCLING, TABLE 1), which can be tracked using STED in membrane trafficking and recycling during endocytosis and exocytosis. Additionally, mCLING allows imaging of dynamic molecular compositions within synaptic organelles such as vesicles, endosomes and active zones[82]. This important approach has been applied to the study of several biological models, including inner hair cells, yeast, cultured hippocampal neurons and *D. melanogaster* larva.

Super-resolution microscopy of protein organization and vesicle dynamics. Super-resolution microscopy imaging, especially that using STED and STORM, has contributed significantly to our understanding of the molecular organization of synaptic vesicles and the dynamic changes during synaptic activities[68,83–86]. For example, the clustering of vesicular compositions after exocytosis has been studied using STED[87], the high resolving power of which is well suited to image the nanometre synaptic vesicles and their densely packed molecular cargo. In particular, anti-synaptotagmin antibodies were incubated in the cell culture with the aim of observing single vesicles in hippocampal neurons. During fusion with the plasma membrane, the antibodies bind to the intravesicular membrane protein synaptotagmin and are internalized inside the vesicles. The cells are then labelled with Atto 532 dye conjugated to secondary antibodies, with STED images allowing resolution of vesicle localization in individual synaptic boutons (FIG. 7a,b). A comparison of synaptotagmin distribution between the inside of the vesicle and on the plasma membrane surface reveals that synaptotagmin does not diffuse to the plasma membrane after exocytosis but appears to remain clustered inside the vesicles.

STED has been applied to study the regeneration of vesicles for renewed exocytosis, particularly vesicular compositions, in hippocampal neurons and in isolated synaptosomes (synaptic terminals from a neuron) from a rat brain and PC12 cells[88]. For example, two-colour STED is used to follow changes in the composition of key exocytosis proteins in vesicles after exocytosis and endocytosis. The vesicle proteins synaptotagmin and synaptophysin can be simultaneously immunolabelled using the fluorescence probes Atto 647N and Atto 590, respectively, and are found to colocalize in 60–70 nm clusters. Although it appears that exocytosis does not affect vesicle composition, endocytosed vesicles retrieve higher amounts of plasma membrane proteins (particularly the SNAREs syntaxin 1 and SNAP-25) as observed using post-labelling for fluorescence. This STED methodology opens the door to a better understanding of the molecular processes that alter the vesicle and cell membranes, and could lead to knowledge of how changes in the synapse help initiate chemical changes that build into memories.

Although synaptic vesicles can release neurotransmitters spontaneously or under stimulation, it is not clear if the same vesicles are used for release in both modes. A modified approach called isoSTED, which affords 3D resolution of about 40–50 nm, has been used to track vesicles during two cycles of endocytosis and exocytosis to distinguish spontaneous versus stimulated release[69]. The vesicle marker synaptotagmin was double immunolabelled with antibodies that had different fluorescent colours for each release cycle. From the isoSTED images, colocalization of the two colour signals was observed at the same structures, indicating that a synaptic vesicle can participate in both spontaneous and stimulated release. These experiments all involve acquiring snapshots of vesicle locations in fixed tissues at different times.

As has been emphasized above, relative to STORM, STED is a fast imaging method that is applicable to the monitoring of dynamic biological processes in living systems. STED has been used to track the movements of synaptic vesicles in living hippocampal neurons[71]. The locations of single vesicles can be followed by immunolabelling synaptotagmin with antibodies conjugated with Atto 647N. Videos of vesicle movement within an area of 1.8 μm × 2.5 μm have been recorded at 28 frames per second by scanning excitation and depletion beams and moving the sample stage. Taken together, the data show many hotspots where vesicles are immobile, as well as tracks where the vesicles were clearly in motion. About 31% of the vesicles pass through the hotspots, spending an average time of 16% in these regions. It appears that vesicles continuously bind then diffuse away from the cellular organelles in a manner similar to the 'stick and diffuse' model[89] for vesicle trafficking, a mechanism with a function that remains to be elucidated.

Multimodal imaging and electroanalysis

Molecular turnover with STED and nanoSIMS. Combining different imaging techniques enables the collection of complementary data on a single system such as a synapse. Molecular turnover in the synapse is an important process, the mechanism of which has remained elusive because of the high complexity of the synaptic structure and the lack of suitable analytical tools. Synaptic turnover has recently been studied using a correlated approach that combines super-resolution optical STED with nanoSIMS imaging, the latter enabling visualization and quantification of biomolecules labelled with stable isotopes in biological samples[90]. The combined method allows identification of specific organelles and their corresponding isotopic and molecule-specific turnover (metabolism) at high lateral (~50 nm) and depth resolution (~5.7 nm). In these experiments, hippocampal neurons were pulsed in the presence of ^{15}N-leucine, which is incorporated into newly synthesized proteins and as a marker for neuronal turnover. The neurons were also immunostained for different cellular markers, such as synaptophysin I for synaptic vesicles, bassoon protein for the active zones, and TOMM20 for the mitochondria. NanoSIMS enabled the calculation of neuronal turnover according to the ^{15}N/^{14}N ratio, and it was shown that the molecular

© 2017 Macmillan Publishers Limited, part of Springer Nature. All rights reserved.

turnover rate of the synapse is higher than other areas in the neuronal axon (FIG. 7d–f). In summary, this protocol will undoubtedly be a very powerful approach for the study of molecular turnover of other organelles and biological systems.

The advantages of the correlated approach have also been realized using a new method for specific protein isotopic and fluorescence labelling[91,92]. Genetic code expansion, followed by click chemistry attachment of isotopic labels, represents a flexible and highly specific approach to tag any protein of interest, which can then be visualized using both STED and nanoSIMS. The labelling approach involves incorporating unnatural amino acids into a protein, which is then coupled to a small molecule containing a fluorophore and ^{19}F atoms. Correlating STED and nanoSIMS images, which highlight fluorescence and ^{19}F concentration, respectively, allows the identification of regions in which these signals overlap, and this multimodal turnover analysis can be performed at a range of different cellular structures.

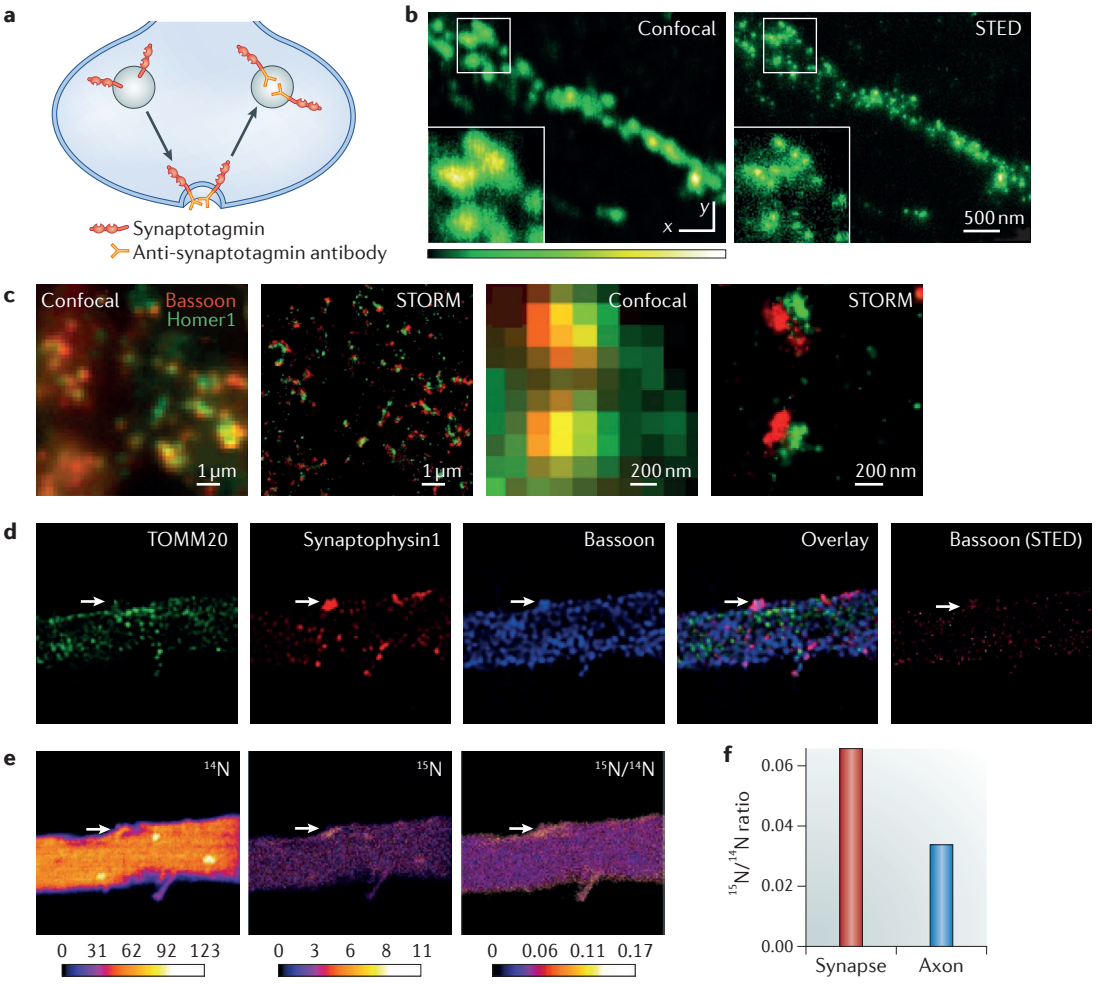

Figure 7 | **Applications of super-resolution STED, STORM and nanoSIMS imaging in synaptic research. a,b** | STED imaging of synaptic vesicles in cultured hippocampal neurons. **a** | Schematic illustration of vesicle labelling. Exocytosis allows the vesicular protein synaptotagmin to bind to anti-synaptotagmin antibodies, which are internalized during endocytosis. **b** | Comparing confocal and STED micrographs of the synaptic terminal immunostained with Atto-532-labelled anti-synaptotagmin antibodies emphasizes the superior spatial resolving power of STED. **c** | STORM imaging of presynaptic Bassoon and postsynaptic Homer1 proteins in a glomerulus at a mouse main olfactory bulb. Bassoon and Homer1 were immunolabelled with antibodies containing Cy3-Atto 647 and Atto 405–Atto 647, respectively. The overlapping structures observed in confocal micrographs are clearly resolved using STORM. **d–f** | Correlated STED and nanoSIMS imaging of neuronal axons of hippocampal neurons. **d** | Confocal images of the mitochondrial marker TOMM20, synaptic vesicle synaptophysin I, active zone Bassoon and their overlaid image. Bassoon imaged by STED shows more detailed localization. The arrowheads indicate the synapse where all the markers overlap. **e** | SIMS images of the same axonal area for the isotopes ^{14}N, ^{15}N, and the ratio $^{15}N/^{14}N$. **f** | NanoSIMS allows mapping of $^{15}N/^{14}N$ ratios. Indicative of high protein turnover, these values are greatest for synaptic regions relative to other regions in the axon. SIMS, secondary ion mass spectrometry; STED, stimulated emission depletion; STORM, stochastic optical reconstruction microscopy. Panels **a** and **b** are adapted and reproduced, respectively, with permission from REF. 87, Macmillan Publishers Limited. Panel **c** is adapted with permission from REF. 68, Cell Press. Panels **d–f** are reproduced with permission from REF. 90, Macmillan Publishers Limited.

© 2017 Macmillan Publishers Limited, part of Springer Nature. All rights reserved.

Structure and activity with STED, electron microscopy and quantitative mass spectrometry. Combining super-resolution microscopy and electron microscopy (EM) imaging with quantitative mass spectrometry has proved useful in studying the structure and activity of synapses and vesicles. Such multimodal analysis allows investigation of protein organization within the synapse and synaptic vesicles. In particular, immunoblotting and mass spectrometry quantifies the relative amounts of major proteins; EM determines the position, size and number of organelles; and STED measures protein positions[70]. Synaptosomes were purified and subjected to mass spectrometry to determine protein molecular weights. Combined with immunoblotting, which is used to measure the total mass of each protein in each synaptosome, it is possible to know the number of each protein molecule present, the 'copy number'. Overall, sixty-two synaptic proteins were analysed, with those performing the same synaptic function being present in similar molar quantities. For example, proteins related to vesicle fusion, such as the SNAREs, have ~20,000–26,000 copies per vesicle. By contrast, the mean copy numbers of the endocytosis proteins clathrin and dynamin per synapse are only about 4,000 and 2,300, respectively. Proteins used for exocytosis are found to be more abundant than those for endocytosis because the high speed of exocytosis requires a large number of regulatory proteins. Another explanation might be that most exocytosis events are not followed by traditional endocytosis, but rather involve partial release and immediate vesicle recapture. To correlate the copy number with the synaptic function of proteins, EM and STED are useful in providing morphological information and locations of proteins in 3D space within the synapse. The detailed maps of protein organization that are generated indicate that synaptic vesicles occupy most of the space in the synaptosome, with proteins mainly being localized where they function (FIG. 8a,b).

Combinations of super-resolution fluorescence imaging with other imaging techniques have been used to determine the locations of specific proteins in biological tissue and cells. For example, STED and PALM fluorescence nanoscopy, together with EM, have been used to pinpoint proteins in *Caenorhabditis elegans*[93], whereas STED and EM reveal the organization and functions of the Bruchpilot protein in the active zone assembly in *D. melanogaster*[94]. Also notable is the combination of 3D STORM and EM, which can be used to image different cellular substructures[95]. These combinations of analytical techniques also appear highly suitable for the imaging of synaptic vesicles, although no such studies have yet been reported.

Location and kinetics with nanoSIMS, single-cell amperometry and intracellular VIEC. NanoSIMS, transmission electron microscopy (TEM), single-cell amperometry and intramolecular VIEC have been used to visualize and understand dopamine content and distribution across single vesicles. In this way, the vesicle content can be quantified, while simultaneously evaluating the kinetics of dopamine transfer between two vesicular compartments: the halo (solution surrounding protein matrix) and the dense core[96]. PC12 cells were incubated with the dopamine precursor ^{13}C-L-DOPA to visualize newly synthesized dopamine in the vesicles. NanoSIMS and TEM analyses enabled identification of cellular features including vesicles (and their protein-rich dense cores), in which enrichment of ^{13}C dopamine was observed (FIG. 8c). The dynamics of loading dopamine into vesicles were examined under different conditions, including treatments with ^{13}C-L-DOPA and the administration of reserpine, a drug used to deplete dopamine from vesicles. The data for vesicle content obtained from nanoSIMS were compared with those obtained by intracellular VIEC, as well as to the amount of dopamine released measured by single-cell amperometry. Indeed, reserpine was found to deplete the ^{13}C-enriched dopamine following ^{13}C-L-DOPA loading, although the process is reversible in that enrichment could be retained after ^{13}C-L-DOPA reloading. Dopamine storage in and removal from vesicles were also examined for short and long ^{13}C-L-DOPA incubation periods. The depletion of enrichment by reserpine was less significant for long incubation times, which can be rationalized by considering that longer incubation times lead to higher dopamine enrichment inside the protein dense core. Owing to the slow kinetics of catecholamine transfer between the dense core matrix and the surrounding solution, a higher amount of dopamine appears to be retained after long ^{13}C-L-DOPA incubation and treatment with reserpine. This is supported by correlating TEM and nanoSIMS images of single vesicles, which revealed the distributions of enriched dopamine within the vesicular nanocompartments under different conditions. NanoSIMS images of the vesicle interiors were used to show that short L-DOPA incubation times lead to dopamine primarily being in the halo, whereas longer incubation times result in more dopamine localizing in the dense core (FIG. 8d). Overall, it appears that the movement of transmitters between nanocompartments of intact vesicles is kinetically limited, possibly on a timescale of hours.

Conclusion and outlook

Improvements in analytical instrumentation and chemical analyses have enabled measurements of several aspects of single vesicles and sub-vesicular regions. As highlighted in this Review, *in vivo* amperometry and intracellular VIEC provide the ability to quantify the amount of transmitter released and the total content in individual vesicles, respectively. Conventional techniques have been used to measure the amount released from vesicles during exocytosis, which may proceed by full release distension, partial release, kiss and run, or flickering. Although the mechanisms operative during exocytosis events are still under debate, recent intracellular VIEC studies in live cells strongly suggest that partial releases of vesicle transmitters are the predominant exocytosis events.

Super-resolution microscopic imaging enables the observation of fluorophore tags within a vesicle and the determination of synaptic activity during vesicle recycling. Nanoscale isotopic imaging with nanoSIMS

© 2017 Macmillan Publishers Limited, part of Springer Nature. All rights reserved.

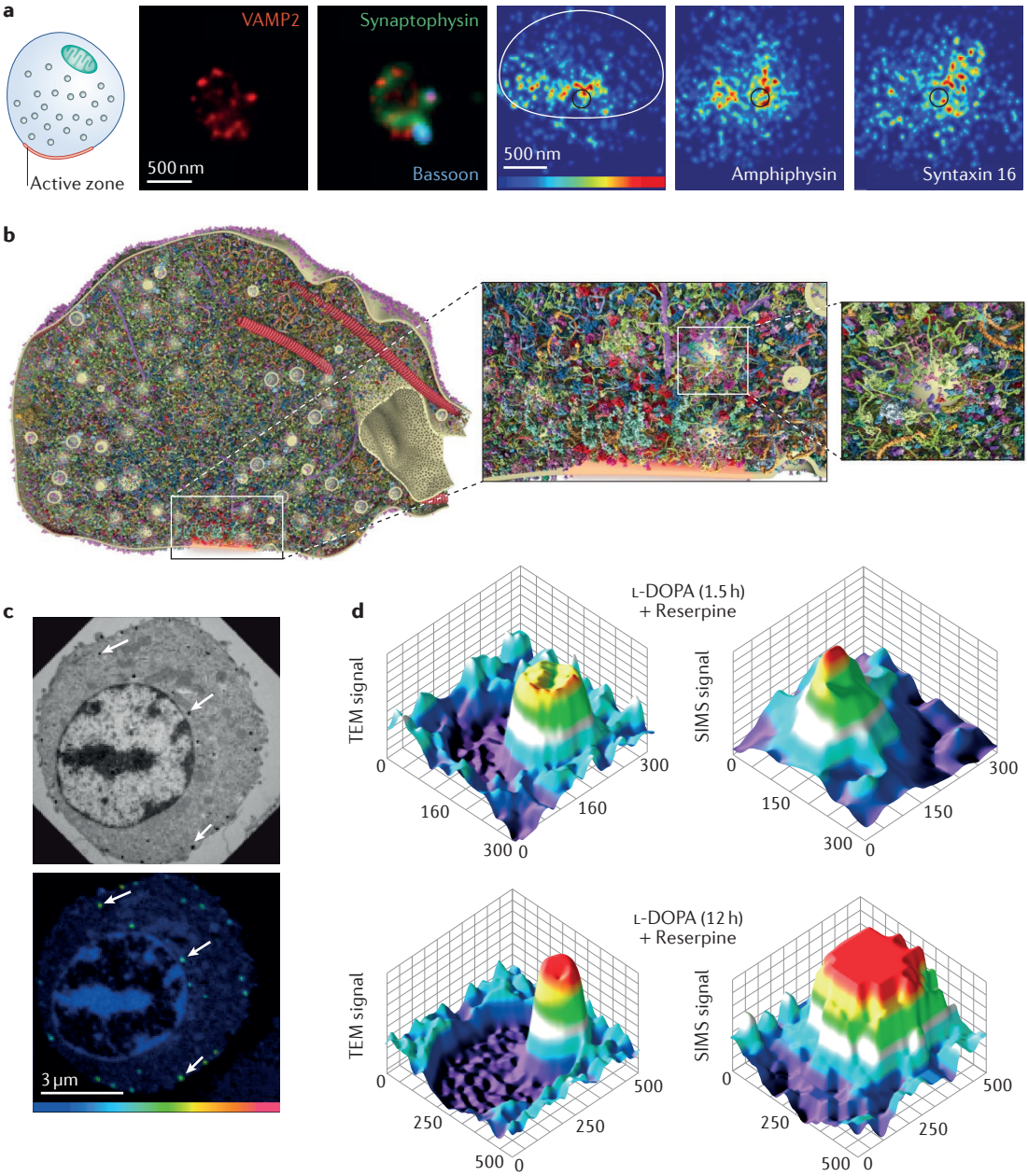

Figure 8 | **Multimodal molecular imaging uncovers the structure and synaptic activity of single vesicles. a**,**b** | The organization of proteins within the synaptosome and vesicles can be determined using multimodal analysis. Such a study can include immunoplotting and mass spectrometry for protein quantification, electron microscopy (EM) for morphology analysis, and STED for protein localization. **a** | Protein organization of a synaptosome. The schematic illustration on the left is of a synaptosome containing an active zone and vesicles. The synaptosome was immunolabelled for the protein of interest VAMP2 (imaged by STED), for active zone Bassoon and for the vesicle protein synaptophysin (imaged by confocal microscopy). The last three panels show the relative density distribution of VAMP2, presynaptic amphiphysin-containing vesicle and syntaxin 16 in the synapse. The relative abundance is colour coded. **b** | The 3D organization of 60 different synaptic proteins at a synaptosome, active zone and a vesicle. **c**,**d** | Multimodal imaging of dopamine across synaptic vesicles. **c** | TEM (top) and nanoSIMS (bottom) images of PC12 cells incubated with ^{13}C-L-DOPA. By using nanoSIMS to map the $^{13}C^{14}N/^{12}C^{14}N$ ratio, the enrichment of ^{13}C through newly synthesized dopamine inside the vesicles (arrows) can be studied. **d** | Correlation of 3D plots of TEM data and nanoSIMS $^{13}C^{14}N$ L-DOPA ion intensities from a single vesicle. Data are collected after 1.5 h (top) or 12 h (bottom) incubation with L-DOPA. Intense (yellow or red) regions in the TEM data are assigned to dense core proteins, around which is a protein matrix halo (dark blue). For the nanoSIMS image, the red and dark blue indicate high and low ^{13}C enrichment, respectively. Longer incubation with L-DOPA results in more dopamine being localized in the dense core. SIMS, secondary ion mass spectrometry; STED, stimulated emission depletion; TEM, transmission electron microscopy. Panels **a** and **b** are reproduced and adapted, respectively, with permission from REF. 70, AAAS. Panels **c** and **d** are adapted with permission from REF. 96, American Chemical Society.

© 2017 Macmillan Publishers Limited, part of Springer Nature. All rights reserved.

can be used to visualize molecular turnover in nanometre-size single vesicles. Moreover, the development of isotopic and fluorescence labelling has made the combination of super-resolution optical and isotopic imaging a particularly powerful approach to correlate synaptic structure and isotopic turnover. Alternatively, the combination of nanoSIMS with cellular electrochemistry provides a new means to relate vesicle activity to structure. Multimodal approaches with these advanced technologies have greatly broadened the scope of possibilities in the research of synaptic vesicles. Even so, researchers using these techniques face several challenges, not least the narrow range of molecules detectable with cellular electrochemistry. Although significant improvements to biosensors have been made, there is a great deal of work to be done to develop faster, more sensitive and smaller electrodes necessary for measurements of the present type. Super-resolution microscopy now enables multicolour 3D imaging with nanoscale lateral and depth resolution, and live imaging of dynamic molecular processes inside biological systems with high temporal and spatial resolution. Imaging with molecular resolving power will become more useful as smaller, brighter and more photostable fluorescence probes are discovered. Furthermore, flexible and biologically friendly superprobes and sample preparations are being developed to facilitate multimodal imaging. With improved technology and methodology, cellular electrochemistry and nanoscale molecular imaging will soon promise to significantly expand our understanding of nanobiological structures and functions, including the synapse and vesicles.

1. Takamori, S. *et al.* Molecular anatomy of a trafficking organelle. *Cell* **127**, 831–846 (2006).
2. Cox, H. D. & Thompson, C. M. Purification and proteomic analysis of synaptic vesicles. *Methods Mol. Biol.* **432**, 259–274 (2008).
3. Zito, K., Parnas, D., Fetter, R. D., Isacoff, E. Y. & Goodman, C. S. Watching a synapse grow: noninvasive confocal imaging of synaptic growth in *Drosophila*. *Neuron* **22**, 719–729 (1999).
4. Stevens, B. *et al.* The classical complement cascade mediates CNS synapse elimination. *Cell* **131**, 1164–1178 (2007).
5. Li, X., Dunevall, J. & Ewing, A. G. Quantitative chemical measurements of vesicular transmitters with electrochemical cytometry. *Acc. Chem. Res.* **49**, 2347–2354 (2016).
6. Wightman, R. M. *et al.* Temporally resolved catecholamine spikes correspond to single vesicle release from individual chromaffin cells. *Proc. Natl Acad. Sci. USA* **88**, 10754–10758 (1991).
This paper describes one of the earliest amperometric measurements of catecholamines released during exocytosis.
7. Mellander, L. J. *et al.* Two modes of exocytosis in an artificial cell. *Sci. Rep.* **4**, 3847–3853 (2014).
8. Omiatek, D. M., Dong, Y., Heien, M. L. & Ewing, A. G. Only a fraction of quantal content is released during exocytosis as revealed by electrochemical cytometry of secretory vesicles. *ACS Chem. Neurosci.* **1**, 234–245 (2010).
The authors of this article demonstrated experimentally that exocytosis is mostly 'open and closed' or partial release.
9. Fernandez-Suarez, M. & Ting, A. Y. Fluorescent probes for super-resolution imaging in living cells. *Nat. Rev. Mol. Cell Biol.* **9**, 929–943 (2008).
10. Pihel, K., Schroeder, T. J. & Wightman, R. M. Rapid and selective cyclic voltammetric measurements of epinephrine and norepinephrine as a method to measure secretion from single bovine adrenal medullary cells. *Anal. Chem.* **66**, 4532–4537 (1994).
11. Betz, W. J., Mao, F. & Smith, C. B. Imaging exocytosis and endocytosis. *Curr. Opin. Neurobiol.* **6**, 365–371 (1996).
12. Cahill, P. S. *et al.* Microelectrodes for the measurement of catecholamines in biological systems. *Anal. Chem.* **68**, 3180–3186 (1996).
13. Travis, E. R. & Wightman, R. M. Spatio-temporal resolution of exocytosis from individual cells. *Annu. Rev. Biophys. Biomol. Struct.* **27**, 77–103 (1998).
14. Aravanis, A. M., Pyle, J. L., Harata, N. C. & Tsien, R. W. Imaging single synaptic vesicles undergoing repeated fusion events: kissing, running, and kissing again. *Neuropharmacology* **45**, 797–813 (2003).
15. Jin, H., Heller, D. A. & Strano, M. S. Single-particle tracking of endocytosis and exocytosis of single-walled carbon nanotubes in NIH-3T3 cells. *Nano Lett.* **8**, 1577–1585 (2008).
16. Xia, X. F., Lessmann, V. & Martin, T. F. J. Imaging of evoked dense-core-vesicle exocytosis in hippocampal neurons reveals long latencies and kiss-and-run fusion events. *J. Cell Sci.* **122**, 75–82 (2009).
17. Leszczyszyn, D. J. *et al.* Nicotinic receptor-mediated catecholamine secretion from individual chromaffin cells: chemical evidence for exocytosis. *J. Biol. Chem.* **265**, 14736–14737 (1990).
18. Amatore, C. *et al.* Relationship between amperometric pre-spike feet and secretion granule composition in chromaffin cells: an overview. *Biophys. Chem.* **129**, 181–189 (2007).
19. Chow, R. H., von Rüden, L. & Neher, E. Delay in vesicle fusion revealed by electrochemical monitoring of single secretory events in adrenal chromaffin cells. *Nature* **356**, 60–63 (1992).
20. De Toledo, G. A., Fernández-Chacón, R. & Fernández, J. M. Release of secretory products during transient vesicle fusion. *Nature* **363**, 554–558 (1993).
21. Ren, L. *et al.* The evidence for open and closed exocytosis as the primary release mechanism. *Q. Rev. Biophys.* **49**, e12 (2016).
22. Amatore, C., Oleinick, A. I. & Svir, I. Reconstruction of aperture functions during full fusion in vesicular exocytosis of neurotransmitters. *ChemPhysChem* **11**, 159–174 (2010).
23. Dunevall, J. *et al.* Characterizing the catecholamine content of single mammalian vesicles by collision–adsorption events at an electrode. *J. Am. Chem. Soc.* **137**, 4344–4346 (2015).
This work demonstrated that it is possible to count molecules in vesicles that undergo stochastic collisions at an electrode, followed by adsorption and opening.
24. Li, X., Majdi, S., Dunevall, J., Fathali, H. & Ewing, A. G. Quantitative measurement of transmitters in individual vesicles in the cytoplasm of single cells with nanotip electrodes. *Angew. Chem. Int. Ed.* **54**, 11978–11982 (2015).
Demonstration of intracellular VIEC for vesicle content in live cells.
25. Bruns, D. & Jahn, R. Real-time measurement of transmitter release from single synaptic vesicles. *Nature* **377**, 62–65 (1995).
26. Staal, R. G., Mosharov, E. V. & Sulzer, D. Dopamine neurons release transmitter via a flickering fusion pore. *Nat. Neurosci.* **7**, 341–346 (2004).
27. Mellander, L. J., Trouillon, R., Svensson, M. I. & Ewing, A. G. Amperometric post spike feet reveal most exocytosis is via extended kiss-and-run fusion. *Sci. Rep.* **2**, 907 (2012).
28. Chen, Y. A. & Scheller, R. H. SNARE-mediated membrane fusion. *Nat. Rev. Mol. Cell Biol.* **2**, 98–106 (2001).
29. Feany, M. B. & Bender, W. W. A. *Drosophila* model of Parkinson's disease. *Nature* **404**, 394–398 (2000).
30. Finelli, A., Kelkar, A., Song, H. J., Yang, H. & Konsolaki, M. A model for studying Alzheimer's Aβ42-induced toxicity in *Drosophila melanogaster*. *Mol. Cell. Neurosci.* **26**, 365–375 (2004).
31. Watson, M. R., Lagow, R. D., Xu, K., Zhang, B. & Bonini, N. M. A. *Drosophila* model for amyotrophic lateral sclerosis reveals motor neuron damage by human SOD1. *J. Biol. Chem.* **283**, 24972–24981 (2008).
32. Majdi, S. *et al.* Electrochemical measurements of optogenetically stimulated quantal amine release from single nerve cell varicosities in *Drosophila* larvae. *Angew. Chem. Int. Ed.* **54**, 13609–13612 (2015).
This article describes amperometric measurement of exocytosis from single neurons in *D. melanogaster*.
33. Li, Y.-T. et al. Real-time monitoring of discrete synaptic release events and excitatory potentials within self-reconstructed neuromuscular junctions. *Angew. Chem. Int. Ed.* **54**, 9313–9318 (2015).
34. Li, Y.-T. *et al.* Nanoelectrode for amperometric monitoring of individual vesicular exocytosis inside single synapses. *Angew. Chem. Int. Ed.* **53**, 12456–12460 (2014).
A report on the use of nanotip electrodes to measure noradrenaline release inside a nanometre synapse.
35. Strein, T. G. & Ewing, A. G. Characterization of submicron-sized carbon electrodes insulated with a phenol–allylphenol copolymer. *Anal. Chem.* **64**, 1368–1373 (1992).
36. Borges, R., Travis, E. R., Hochstetler, S. E. & Wightman, R. M. Effects of external osmotic pressure on vesicular secretion from bovine adrenal medullary cells. *J. Biol. Chem.* **272**, 8325–8331 (1997).
37. Camacho, M., Machado, J. D., Montesinos, M. S., Criado, M. & Borges, R. Intragranular pH rapidly modulates exocytosis in adrenal chromaffin cells. *J. Neurochem.* **96**, 324–334 (2006).
38. Haynes, C. L., Siff, L. N. & Wightman, R. M. Temperature-dependent differences between readily releasable and reserve pool vesicles in chromaffin cells. *Biochim. Biophys. Acta* **1773**, 728–735 (2007).
39. Machado, J. D., Morales, A., Gomez, J. F. & Borges, R. cAMP modulates exocytotic kinetics and increases quantal size in chromaffin cells. *Mol. Pharmacol.* **60**, 514–520 (2001).
40. Calvo-Gallardo, E. *et al.* Faster kinetics of quantal catecholamine release in mouse chromaffin cells stimulated with acetylcholine, compared with other secretagogues. *J. Neurochem.* **139**, 722–736 (2016).
41. Pothos, E. N. *et al.* Stimulation-dependent regulation of the pH, volume and quantal size of bovine and rodent secretory vesicles. *J. Physiol.* **542**, 453–476 (2002).
42. Elhamdani, A., Palfrey, H. C. & Artalejo, C. R. Quantal size is dependent on stimulation frequency and calcium entry in calf chromaffin cells. *Neuron* **31**, 819–830 (2001).
43. Sombers, L. A., Maxson, M. M. & Ewing, A. G. Loaded dopamine is preferentially stored in the halo portion of PC12 cell dense core vesicles. *J. Neurochem.* **93**, 1122–1131 (2005).
44. Omiatek, D. M., Santillo, M. F., Heien, M. L. & Ewing, A. G. Hybrid capillary-microfluidic device for the separation, lysis, and electrochemical detection of vesicles. *Anal. Chem.* **81**, 2294–2302 (2009).
45. Omiatek, D. M. *et al.* The real catecholamine content of secretory vesicles in the CNS revealed by electrochemical cytometry. *Sci. Rep.* **3**, 1447–1452 (2013).
46. Cheng, W. & Compton, R. G. Investigation of single-drug-encapsulating liposomes using the nano-impact method. *Angew. Chem. Int. Ed.* **53**, 13928–13930 (2014).

© 2017 Macmillan Publishers Limited, part of Springer Nature. All rights reserved.

47. Lovrić, J. *et al.* On the mechanism of electrochemical vesicle cytometry: chromaffin cell vesicles and liposomes. *Faraday Discuss.* **193**, 65–79 (2016).
48. Trouillon, R. & Ewing, A. G. Actin controls the vesicular fraction of dopamine released during extended kiss and run exocytosis. *ACS Chem. Biol.* **9**, 812–820 (2014).
49. Najafinobar, N. *et al.* Excited fluorophores enhance the opening of vesicles at electrode surfaces in vesicle electrochemical cytometry. *Angew. Chem. Int. Ed.* **55**, 15081–15085 (2016).
50. Lebègue, E., Anderson, C. M., Dick, J. E., Webb, L. J. & Bard, A. J. Electrochemical detection of single phospholipid vesicle collisions at a Pt ultramicroelectrode. *Langmuir* **31**, 11734–11739 (2015).
51. Cheng, W. & Compton, R. G. Measuring the content of a single liposome through electrocatalytic nanoimpact "titrations". *ChemElectroChem* **3**, 2017–2020 (2016).
52. Li, X., Dunevall, J. & Ewing, A. G. Using single-cell amperometry to reveal how cisplatin treatment modulates the release of catecholamine transmitters during exocytosis. *Angew. Chem. Int. Ed.* **55**, 9041–9044 (2016).
53. Ren, L. *et al.* Zinc regulates chemical-transmitter storage in nanometer vesicles and exocytosis dynamics as measured by amperometry. *Angew. Chem. Int. Ed.* **56**, 4970–4975 (2017).
54. Colliver, T. L., Pyott, S. J., Achalabun, M. & Ewing, A. G. VMAT-mediated changes in quantal size and vesicular volume. *J. Neurosci.* **20**, 5276–5282 (2000).
55. Fathali, H., Dunevall, J., Majdi, S. & Cans, A.-S. Extracellular osmotic stress reduces the vesicle size while keeping a constant neurotransmitter concentration. *ACS Chem. Neurosci.* **8**, 368–375 (2017).
56. Huang, B., Bates, M. & Zhuang, X. Super-resolution fluorescence microscopy. *Annu. Rev. Biochem.* **78**, 993–1016 (2009).
57. Hell, S. W. & Wichmann, J. Breaking the diffraction resolution limit by stimulated emission: stimulated-emission-depletion fluorescence microscopy. *Opt. Lett.* **19**, 780–782 (1994).
58. Hein, B., Willig, K. I. & Hell, S. W. Stimulated emission depletion (STED) nanoscopy of a fluorescent protein-labeled organelle inside a living cell. *Proc. Natl Acad. Sci. USA* **105**, 14271–14276 (2008).
59. Moneron, G. & Hell, S. W. Two-photon excitation STED microscopy. *Opt. Express* **17**, 14567–14583 (2009).
60. Neupane, B., Ligler, F. S. & Wang, G. Review of recent developments in stimulated emission depletion microscopy: applications on cell imaging. *J. Biomed. Opt.* **19**, 080901 (2014).
61. Török, P. & Munro, P. R. T. The use of Gauss–Laguerre vector beams in STED microscopy. *Opt. Express* **12**, 3605–3617 (2004).
62. Kotlyar, V. V., Almazov, A. A., Khonina, S. N. & Soifer, V. A. Generation of phase singularity through diffracting a plane or Gaussian beam by a spiral phase plate. *J. Opt. Soc. Am. A* **22**, 849–861 (2005).
63. Schmidt, R. *et al.* Spherical nanosized focal spot unravels the interior of cells. *Nat. Methods* **5**, 539–544 (2008).
64. Curdt, F. *et al.* isoSTED nanoscopy with intrinsic beam alignment. *Opt. Express* **23**, 30891–30903 (2015).
65. Rust, M. J., Bates, M. & Zhuang, X. Sub-diffraction-limit imaging by stochastic optical reconstruction microscopy (STORM). *Nat. Methods* **3**, 793–795 (2006).
66. Betzig, E. *et al.* Imaging intracellular fluorescent proteins at nanometer resolution. *Science* **313**, 1642–1645 (2006).
67. Xu, K., Babcock, H. P. & Zhuang, X. Dual-objective STORM reveals three-dimensional filament organization in the actin cytoskeleton. *Nat. Methods* **9**, 185–188 (2012).
68. Dani, A., Huang, B., Bergan, J., Dulac, C. & Zhuang, X. Superresolution imaging of chemical synapses in the brain. *Neuron* **68**, 843–856 (2010).
69. Wilhelm, B. G., Groemer, T. W. & Rizzoli, S. O. The same synaptic vesicles drive active and spontaneous release. *Nat. Neurosci.* **13**, 1454–1456 (2010).
70. Wilhelm, B. G. *et al.* Composition of isolated synaptic boutons reveals the amounts of vesicle trafficking proteins. *Science* **344**, 1023–1028 (2014).
This report describes protein organization of the synaptic bouton and vesicle, including a 3D model of synaptic structure.
71. Westphal, V. *et al.* Video-rate far-field optical nanoscopy dissects synaptic vesicle movement. *Science* **320**, 246–249 (2008).
72. Huang, B., Wang, W., Bates, M. & Zhuang, X. Three-dimensional super-resolution imaging by stochastic optical reconstruction microscopy. *Science* **319**, 810–813 (2008).
The first demonstration of 3D imaging using STORM, applied here to observe the structure of protein microtubules and clathrin-coated pits in cells.
73. Balzarotti, F. *et al.* Nanometer resolution imaging and tracking of fluorescent molecules with minimal photon fluxes. *Science* **355**, 606–612 (2017).
This paper describes MINFLUX, a STED variant that minimizes the emitter photons needed for locating single molecules to 1 nm precision. This may allow the study of dynamics, distribution and structure of single molecules in living cells.
74. Opazo, F. *et al.* Aptamers as potential tools for super-resolution microscopy. *Nat. Methods* **9**, 938–939 (2012).
75. Tanaka, K. A. K. *et al.* Membrane molecules mobile even after chemical fixation. *Nat. Methods* **7**, 865–866 (2010).
76. Ries, J., Kaplan, C., Platonova, E., Eghlidi, H. & Ewers, H. A simple, versatile method for GFP-based super-resolution microscopy via nanobodies. *Nat. Methods* **9**, 582–584 (2012).
77. Pleiner, T. *et al.* Nanobodies: site-specific labeling for super-resolution imaging, rapid epitope-mapping and native protein complex isolation. *eLife* **4**, e11349 (2015).
78. Szymborska, A. *et al.* Nuclear pore scaffold structure analyzed by super-resolution microscopy and particle averaging. *Science* **341**, 655–658 (2015).
79. Vreja, I. C. *et al.* Super-resolution microscopy of clickable amino acids reveals the effects of fluorescent protein tagging on protein assemblies. *ACS Nano* **9**, 11034–11041 (2015).
80. Plass, T., Milles, S., Koehler, C., Schultz, C. & Lemke, E. A. Genetically encoded copper-free click chemistry. *Angew. Chem. Int. Ed.* **50**, 3878–3881 (2011).
81. de Castro, M. A., Rammner, B. & Opazo, F. Aptamer stainings for super-resolution microscopy. *Methods Mol. Biol.* **1380**, 197–210 (2016).
82. Revelo, N. H. *et al.* A new probe for super-resolution imaging of membranes elucidates trafficking pathways. *J. Cell Biol.* **205**, 591–606 (2014).
83. Jung, S. *et al.* Disruption of adaptor protein 2μ (AP-2μ) in cochlear hair cells impairs vesicle reloading of synaptic release sites and hearing. *EMBO J.* **34**, 2686–2702 (2015).
84. Opazo, F. *et al.* Limited intermixing of synaptic vesicle components upon vesicle recycling. *Traffic* **11**, 800–812 (2010).
85. Spuhler, I. A., Conley, G. M., Scheffold, F. & Sprecher, S. G. Super resolution imaging of genetically labeled synapses in *Drosophila* brain tissue. *Front. Cell. Neurosci.* **10**, 142 (2016).
86. Pech, U., Revelo, N. H., Seitz, K. J., Rizzoli, S. O. & Fiala, A. Optical dissection of experience-dependent pre- and postsynaptic plasticity in the *Drosophila* brain. *Cell Rep.* **10**, 2083–2095 (2015).
87. Willig, K. I., Rizzoli, S. O., Westphal, V., Jahn, R. & Hell, S. W. STED microscopy reveals that synaptotagmin remains clustered after synaptic vesicle exocytosis. *Nature* **440**, 935–939 (2006).
This article considers the nature of vesicular membrane protein synaptotagmin I during vesicle recycling using STED.
88. Hoopmann, P. *et al.* Endosomal sorting of readily releasable synaptic vesicles. *Proc. Natl Acad. Sci. USA* **107**, 19055–19060 (2010).
89. Yeung, C., Shtrahman, M. & Wu, X.-L. Stick-and-diffuse and caged diffusion: a comparison of two models of synaptic vesicle dynamics. *Biophys. J.* **92**, 2271–2280 (2007).
90. Saka, S. K. *et al.* Correlated optical and isotopic nanoscopy. *Nat. Commun.* **5**, 3664 (2014).
91. Vreja, I. C. *et al.* Secondary-ion mass spectrometry of genetically encoded targets. *Angew. Chem. Int. Ed.* **54**, 5784–5788 (2015).
92. Kabatas, S. *et al.* A contamination-insensitive probe for imaging specific biomolecules by secondary ion mass spectrometry. *Chem. Commun.* **51**, 13221–13224 (2015).
93. Watanabe, S. *et al.* Protein localization in electron micrographs using fluorescence nanoscopy. *Nat. Methods* **8**, 80–84 (2011).
94. Fouquet, W. *et al.* Maturation of active zone assembly by *Drosophila* Bruchpilot. *J. Cell Biol.* **186**, 129–145 (2009).
95. Kim, D. *et al.* Correlative stochastic optical reconstruction microscopy and electron microscopy. *PLoS ONE* **10**, e0124581 (2015).
96. Lovrič, J. *et al.* Nano secondary ion mass spectrometry imaging of dopamine distribution across nanometer vesicles. *ACS Nano* **11**, 3446–3455 (2017).
The paper describes applications of multimodal nanoSIMS, TEM and single-cell electrochemistry to image single vesicles and quantify neurotransmitter content and release. The results implicate a role for vesicle inner structure on regulating release kinetics.
97. Dean, K. M. & Palmer, A. E. Advances in fluorescence labeling strategies for dynamic cellular imaging. *Nat. Chem. Biol.* **10**, 512–523 (2014).

Acknowledgements
The authors thank S. O. Rizzoli for helpful comments, and the many colleagues and collaborators that have contributed to work cited in this Review. This work was supported by the Knut and Alice Wallenberg Foundation, the Swedish Research Council, the European Research Council, and the US National Institutes of Health.

Competing interests statement
The authors declare no competing interests.

Publisher's note
Springer Nature remains neutral with regard to jurisdictional claims in published maps and institutional affiliations.

How to cite this article
Phan, N. T. N., Li, X. & Ewing, A. G. Measuring synaptic vesicles using cellular electrochemistry and nanoscale molecular imaging. *Nat. Rev. Chem.* **1**, 0048 (2017).

© 2017 Macmillan Publishers Limited, part of Springer Nature. All rights reserved.